UNIVERSITI PUTRA MALAYSIA

AERODYNAMICS EFFECT OF COMPUTATIONAL FLUID DYNAMICS APPROACH ON DIFFERENT PROPELLER BLADE DESIGN SUBJECTED TO ORIGIN POSITION

AHMAD FARIDUDDIN BIN AHMAD FARIS

FK 2022 18

AERODYNAMICS EFFECT OF COMPUTATIONAL FLUID DYNAMICS APPROACH ON DIFFERENT PROPELLER BLADE DESIGN SUBJECTED TO ORIGIN POSITION

By

AHMAD FARIDUDDIN BIN AHMAD FARIS

Thesis Submitted to the School of Graduate Studies, Universiti Putra Malaysia, in Fulfilment of the Requirements for the Degree of Master of Science

December 2022

Abstract of thesis presented to the Senate of Universiti Putra Malaysia in fulfilment of the requirement for the Degree of Master of Science

AERODYNAMICS EFFECT OF COMPUTATIONAL FLUID DYNAMICS APPROACH ON DIFFERENT PROPELLER BLADE DESIGN SUBJECTED TO ORIGIN POSITION

By

AHMAD FARIDUDDIN AHMAD FARIS

December 2021

Chair : Adi Azriff Basri, PhD
Faculty : Engineering

The current work presents a numerical method investigation of small-scale propeller aerodynamics performance on 4 different shapes of propeller design using Computational Fluid Dynamic (CFD). This study is conducted due to less studies has been conducted in this airfoil's origin position (AOP) in CFD study, limited study was conducted on the aerodynamics performance respected to the change of origin blade position. In this study, the relationship between the changing of each AOP at each station and the aerodynamics performance was investigated using the CFD approach.

The propellers were designed by changing the AOP at each blade station which produced a different design of propeller shape which can be referred to in percentage of 0% AOP, 25% AOP, 50% AOP, 75% AOP, and 100% AOP. Finite Volume Method using ANSYS Fluent 18.2 was used to analyse this analyses. Multiple Reference Frame (MRF) technique was used for the rotation of the propeller subjected to its local reference frame at 3008 revolutions per minute (RPM). The result of thrust, power coefficients and efficiencies were successfully validated with the experimental wind tunnel data and further the study was conducted to analyse the aerodynamics effect of the 4 different propellers design. The 100% AOP generates an improvement in aerodynamics performance in terms of thrust, coefficient of power, and efficiency with 7.473%, -5.587%, and 15.891% with respect to 25% AOP.

The results also showed a better aerodynamics performance compared to the 25% AOP, 50% AOP, and 75% AOP, especially at the advance ratio of 0.799. This has proven that by increasing the position of the blade origin at each station which develop different of propeller design shape has improved the aerodynamic characteristic and performance of the propeller blade. Hence, using the novel technique of CFD analysis can provide a better platform in designing the best aerodynamics propeller blade design before fabricating the actual model of a propeller

Abstrak tesis yang dikemukakan kepada Senat Universiti Putra Malaysia sebagai memenuhi keperluan untuk Ijazah Master Sains

KESAN AERODINAMIK MENGGUNAKAN PENDEKATAN *COMPUTATIONAL FLUID DYANMIC* PADA REKA BENTUK BILAH KIPAS YANG BERBEZA TERTAKLUK KEPADA KEDUDUKAN ASAL

Oleh

AHMAD FARIDUDDIN AHMAD FARIS

Disember 2021

Pengerusi : Adi Azriff Basri, PhD
Fakulti : Kejuruteraan

Kajian ini menerangkan kaedah penyelidikan berangka prestasi aerodinamik bebaling berskala kecil dengan 4 reka bebaling yang berbeza menggunakan Computational Fluid Dynamic (CFD). Kajian ini dijalankan kerana kurang kajian telah dijalankan untuk kedudukan asal aerofil (AOP) dalam kajian CFD, dan juga kurang kajian yang dijalankan mengenai prestasi aerodinamik dengan perubahan kedudukan asal bilah bebaling. Dalam kajian ini, hubungan antara perubahan kedudukan asal setiap aerofil (AOP) di setiap stesen dan prestasi aerodinamik disiasat menggunakan pendekatan CFD.

Aerofil kedudukan asal bebaling akan diubahkan AOP di setiap stesen bebilah yang akan menghasilkan reka bentuk bentuk bebaling yang berbeza yang dapat disebut dalam peratusan 0% AOP, 25% AOP, 50% AOP, 75% AOP, dan 100% AOP. Kaedah Isipadu Terhingga menggunakan ANSYS Fluent 18.2 digunakan untuk menganalisis analisis ini. Teknik Multiple Reference Frame (MRF) digunakan untuk putaran bebaling yang dikenakan pada kerangka acuan lokal pada 3008 putaran per minit (RPM). Hasil tujahan, pekali daya dan kecekapan telah berjaya disahkan dengan data terowong angin eksperimen dan selanjutnya kajian dilakukan untuk menganalisis kesan aerodinamik dari 4 reka bentuk bebaling yang baru. 100% AOP menghasilkan peningkatan dalam prestasi aerodinamik dari segi tujahan, pekali daya, dan kecekapan dengan 7.473%, -5.587%, dan 15.891% berkenaan dengan 25% AOP.

Hasilnya juga menunjukkan prestasi aerodinamik yang lebih baik dibandingkan dengan AOP 25%, AOP 50%, dan AOP 75%, terutama pada nisbah pendahuluan 0.799. Ini telah membuktikan bahawa dengan meningkatkan kedudukan asal bilah di setiap stesen yang mengembangkan bentuk reka bentuk bebaling yang berbeza telah meningkatkan ciri aerodinamik dan prestasi bilah bebaling. Oleh itu, menggunakan teknik analisis CFD

yang baru dapat menyediakan platform yang lebih baik dalam merancang reka bentuk bilah bebaling aerodinamik terbaik sebelum membuat model sebenar bebaling.

ACKNOWLEDGEMENTS

First of all, I would like to thank Allah S.W.T for all His blessings and guidance which allows me to execute this research accordingly for the entire two and a half years. It has been a challenge for me since I did my Master's Degree during the global pandemic and I choose to work when the pandemic started. Alhamdulillah, I managed to finish it.

Next, I would like to express my sincere thanks and gratitude to my supervisor, Dr. Adi Azriff Basri, and his wife Dr. Erni Illyani for their continuous guidance and motivation in helping me to complete my research and thesis. They helped me a lot and always encouraged me to finish my Master's Degree even I am busy working. Did not forget to both my co-supervisor Prof. Ir. Ts. Dr. Mohamed Thariq Haji Hameed Sultan and Dr. Ezanee Giresfor easing my journey to finish this research.

Lastly, I would like to say my deepest thanks and appreciation to my parents Ahmad Faris Abdullah, Putli Nasarin Abd Sahid, Nur Syahida Laila Azmy, my family members, and my close friends who keep me motivated continuously with their support making me complete Master's Degree in Aerospace Engineering.

This thesis was submitted to the Senate of Universiti Putra Malaysia and has been accepted as fulfilment of the requirement for the degree of Master of Science. The members of the Supervisory Committee were as follows:

Adi Azriff bin Basri, PhD
Senior Lecturer
Faculty of Engineering
Universiti Putra Malaysia
(Chairman)

Mohamed Thariq bin Haji Hameed Sultan, PhD
Professor
Faculty of Engineering
Universiti Putra Malaysia
(Member)

Kamarul Arifin bin Ahmad, PhD
Professor
Faculty of Engineering
Universiti Putra Malaysia
(Member)

Ezanee Gires, PhD
Senior Lecturer
Faculty of Engineering
Universiti Putra Malaysia
(Member)

ZALILAH MOHD SHARIFF, PhD
Professor and Dean
School of Graduate Studies
Universiti Putra Malaysia

Date:19 May 2022

Declaration by Members of Supervisory Committee

This is to confirm that:

- the research and the writing of this thesis were done under our supervision;
- supervisory responsibilities as stated in the Universiti Putra Malaysia (Graduate Studies) Rules 2003 (Revision 2015-2016) are adhered to.

Signature:	
Name of Chairman of Supervisory Committee:	Adi Azriff bin Basri
Signature:	
Name of Member of Supervisory Committee:	Mohamed Thariq bin Haji Hameed Sultan
Signature:	
Name of Member of Supervisory Committee:	Kamarul Arifin bin Ahmad
Signature:	
Name of Member of Supervisory Committee:	Ezanee Gires

TABLE OF CONTENTS

LIST OF TABLES

LIST OF FIGURES

LIST OF ABBREVIATIONS

J	Advance Ratio
L	Lift
n	Rotation per second
P	Power
Q	Torque
Re	Reynold Number
T	Thrust
V	Velocity
ρ	Density
ω	Angular Velocity
η	Efficiency
C_P	Coefficient of Power
C_Q	Coefficient of Torque
C_T	Coefficient of Thrust
V_0	Initial Velocity

CHAPTER 1

INTRODUCTION

.

1.1 Overview

In aerospace industry, one thing that have been a hot topic and interesting field is the technology of Unmanned Aerial Vehicle (UAV), which also known as drone. With the revolution of industry 4.0, the UAV technology has become a niche in aerospace sector. UAV can be used in many sectors such as civil, agriculture or even military. According to a statistic from (*Future of Drones: Applications & Uses of Drone Technology in 2021*, n.d.) the shipment of internet of things enterprise UAV of retail has been increased for the past couple of years. In the year 2019, only 12, 900 UAVs were shipped, but in the year 2021 44, 400 UAVs were shipped to the customers. This shows that, the UAVs technology has been widely used and there will be more drones will be used in many sectors in the future.

UAV is classified as an aircraft or a space craft –without a pilot. It can be control by a pilot on the ground or even now with the advancement of technology UAV can be fly by artificial intelligence (AI). The main component of a UAV is someone who controlled it on the ground or a ground controller, a system to communicate the UAV and the pilot which is a controller and a UAV or the aircraft. The pilot or controller can fly the UAVs far away from them or given the limit distance of the UAV.

The first UAVs can be seen during World War 1. Back then, both U.S and France had been working on developing automatic and unmanned airplanes. This is mainly on military. But during 20th century, UAV have been used across many industries and global awareness. UAVs right now have their own race similar to a car race but the drivers are sitting on the ground with goggle on their eyes.

UAVs are designed for certain missions or goals. According to Hazim Shakhatreh et al (2018), UAVs can do specific missions like as sensing and perceiving the environment, analysing, communicating, planning, and decision making utilising on-board computers, and acting, which needs vehicle control algorithms. UAVs are typically employed for risky missions that do not require humans to confront the threat. These missions are for military, civilian, and transportation purposes.

UAVs are used in the military to provide a target and a decoy for opposing missiles and aircraft. It may also be used for reconnaissance, which is the observation of a territory in order to detect hostile or enemy strategic characteristics. UAVs can also be used as combat aircraft. It is capable of launching missiles without the presence of a pilot in the vehicle. The General Atomics MQ-1 Predator is one such example. Many armed forces had employed this lethal gadget for warfare and reconnaissance.

Figure 1.1: General Atomic MQ-1

UAVs are also -used for agriculture, aerial photography, and data collecting in civilian settings. UAVs can be used to spray pesticides and fertilise crops. The DJI AGRAS MG-1S is shown - in Figure 1.2. (DeBusk, 2010) claims that it can be utilised to save lives. It may be utilised for disaster assistance because the United States has numerous tornadoes and typhoons. It can provide early notice to individuals in the alley so that they can rescue themselves.

Figure 1.2: DJI AGRAS MG-1S

UAVs may be used for freight delivery as well as transportation. It can be utilised to distribute supplies in the event of a disaster. It can also deliver freight, although there are certain limitations because UAVs cannot carry a lot of weight.

Figure 1.1 and figure 1.2 represent the two type of UAVs. One of them is fixed wing while another one is rotorcraft. The fixed wing UAVs can be considered as a normal commercial aircraft. The fixed-wing UAV must employ an engine for propulsion in order to fly. This necessitates the use of gasoline and can be costly because the engine cannot be powered by an electrical source. The best and most cost-effective way to fly a UAV is using a propeller or rotorcraft UAV. The use of a battery or a dry cell in a rotorcraft UAV can lower the cost of operating a UAV. However, there are a few trade-offs from using a battery-powered rotorcraft UAVs. It cannot have a great endurance, which means it cannot fly for an extended period of time. It cannot fly as high as a fixed-wing UAV since it only uses a little amount of electricity. UAVs that are using fuel have more energy density compare to a UAVs that are using fuel cells.

A propeller is a type of fan that produces power by revolving. When there is a pressure difference between the forward and back surfaces of the airfoil-shaped blade, rotational motion may be converted into thrust. In order for a multi-rotor UAV to fly, a simple propeller design will be utilised. Two blades are linked to a central hub.

Thrust is created by the spinning of the propeller from the engine or motor to propel the multirotor UAV forward. According to Bernoulli's principle, the acceleration of the airflow results in a decrease in static pressure in front of the blade. Because of the decreased speed towards the back of the propeller, the static pressure will be larger. As a result of the reaction force, the multirotor UAV will be pushed to go forward due to lower pressure at the front. The pressure differential between the propeller's rear and front sections generates thrust force in the forward direction, which overcomes drag. There are numerous characteristics that must be followed in order to create optimal thrust for a propeller. There are a few theories that have been developed to analyse and design propellers.

Many developments and studies have been conducted in order to make the UAV sector more efficient and effective. The propeller design must be explored so that an optimum propeller can be designed. This can also help save fuels or lower the amount of power required for flying. Hence, in this study, the design of the UAV's propulsion system focusing on the changes of blade position origin respected to the aerodynamics performances is conducted using Computational Fluid Dynamics approach.

1.2 Problem statement

There are several methods for designing the UAV's propeller blade. There are two methods: numerical methods and high fidelity methods. One of the high-fidelity methods available is CFD. CFD is utilised because it is an excellent tool for simulating the

efficiency of the blade in comparison to the experimental technique. It can shorten simulation time and save a lot of money as compared to the experimental technique.

Furthermore, there have been few research on utilising CFD to design the propeller blade of a UAV. Previous studies concentrated on a single parameter. For example, the placement of propeller, ducted propeller, and Micro-Air Vehicle. This is an intriguing issue to investigate and debate.

In this study the propeller's efficiency and lift were investigated. The rotational speed of the propeller blade determines the efficiency of the UAV. Improved blade design must be explored in order to enhance the efficiency of UAV propellant systems. The amount of lift generated by a propeller is determined by the engine RPM, the form of the propeller airfoil, the angle of attack of the blades, and the speed of the aircraft (Turner, 2010). The pitch angle, radius, and airfoil design of the blade are all connected in creating more thrust and power. Less study has been conducted in this matter in CFD study, yet limited study was conducted on the aerodynamics performance respected to the change of origin blade position. This is because this change of origin blade position may influence to the improvement propeller efficiency. Hence in this study the investigation of blade design and the performance of the UAV propulsion system will be conducted by using the CFD approach.

1.3 Objective

The objectives of this study are:

a) To develop and validate CFD simulation of a single rotational propeller blade with the experimental data from UIUC and journal manuscript

b) To compare the effects of changing the origin of blade position on thrust, power and its efficiency of the blade.

c) To determine the best design of propeller blade with respect to the changes of origin blade position

1.4 Scope of Study

This project focuses on the design of the propeller with respect to the changes of the origin blade position which will affect the thrust, power and efficiency of the propeller blade. CFD approach was chosen to be used in this study because it is a time and cost efficient compare to experimental approach. Moving frame technique is used with the help of ANSYS FLUENT 18.2 software. The design of the propeller blade is based on the percentage in terms of airfoil origin position (AOP) which represent 0% AOP, 25% AOP, 50% AOP, 75% AOP and 100% AOP. The optimum design will be presented at the end of the project for certain condition.

1.5 Hypothesis

Few assumptions need to be made in this paper and the assumptions are from the result from other papers that had been reviewed.

a) The position of origin will provide the best result for validation for the (Kutty, & Rajendran, 2017) study based on the design data.

b) The change of origin blade position may influence to the improvement propeller efficiency.

c) The increment of percentage position of blades origin will provide higher thrust, power and efficiency.

1.6 Thesis Layout

This thesis contents 5 chapters:

- Chapter 1 provides an overview of Unmanned Aerial Vehicle (UAV) and propeller. The problem statement, objectives and scope of study are presented.
- Chapter 2 presents the previous research on the blade propeller design and evaluation of propeller performance by using experimental and also numerical approach. Literature findings are discussed here to find the gap of the research.
- Chapter 3 describes the methodology used in this research. A chart in summary on how the research is conducted are presented. A thorough explanation on how the research was conducted by using Computational Fluid Dynamics (CFD).
- Chapter 4 presents the validation of current research. New data from improve designs are also discussed.
- Chapter 5 will conclude the research and future works are recommended

CHAPTER 2

LITERATURE REVIEW

2.1 Introduction

Since the first flight of aircraft, the Wright brothers used a propeller to generate thrust for their aircraft. Propeller has been used to move and lift aircraft, helicopters, boats, submarines, and Unmanned Aerial Vehicle (UAV). To date, the discussion regarding the best propeller blade design for optimum aerodynamics performance still be debated among researchers. From the design perspective, the parameters of the airfoil shape, number of blades, blade angle, and angle of twist are important to be considered which affect the shape of the propeller and the aerodynamic characteristic. With the improvement of current technology, a lot of propeller designs can be tested without performing experimental methods that require lots of expensive equipment such as wind tunnel, time, and cost consumption. The novel technique of Computational Fluid Dynamic (CFD) had become the best tool to be used in analysing the aerodynamics characteristic especially in the preliminary design stage of propeller due to its reliable results. Other fields of study which implement the CFD approach in analysing the performance of blade design are marine ships propeller, UAV propeller, and wind turbine propeller in the preliminary design. This indicated the importance of CFD analysis specially to determine the optimum performance of the propeller blade design.

In this chapter, review on propeller blade design is presented in both experimental and CFD analysis of various fields. The propeller blade is discussed in terms of propeller design, working principle, and evaluation performance. On top of that, the application of propellers in UAVs, aircraft, marine ships, and wind turbine blades is also reviewed according to design and analysis. This chapter is organized as follows; for the first section, the propeller operation was discussed here. This includes the mechanism of the propeller in producing thrust power. The second section is focused on the design of the propeller. Finally, the third section is the evaluation of the propeller performance. This section includes experimental methods and numerical methods which is CFD analysis.

2.2 Propeller Working Principal

A propeller is a piece of equipment that consists of two parts which are a hub and blades known as propeller blades (Havill, 1929). The hub is located at the center of the propeller that holds at least two blades with a twisting shape. The propeller blade is made up of a series of the airfoil that grouped with the different plane station. The airfoils may be varied with different chords and angle of attacks which resulted as the angle of twist. The rotational motion of the propeller can be converted into thrust power when there is a pressure difference between the back and front regions of the blade. On the other hand, the rotating propeller itself able to generate power which converted into turbine purposes.

In ensuring the propeller to be lifted, thrust power is the most important element generated by the rotation of the propeller from the engine or motor. Referring to Bernoulli's principle, the acceleration of the airflow causes a reduction of static pressure in front of the airfoil (NASA, 2010). The propeller experienced higher static pressure due to lower speed downstream of the propeller. Hence, lower pressure at the front forced the multi-rotor UAV to move forward due to the effect of the reaction force. The pressure difference between the back and front sections of the propeller created the thrust force in the forward direction and thus overcome drag. The twisting airfoil of propeller blades created a chamber shape that caused the airflow in front of the blade to travel at a higher speed.

2.3 Propeller Blade Design

The design of the propeller blade is categorised into two which are conventional and unconventional. (Kutty & Rajendran, 2017b). The conventional design of the propeller is focused on the airfoil selection, chord of the airfoil, blade angle, blade twist, blade diameter, and blade thickness, as in Figure 2.1. The unconventional design of the propeller is focused on ducted, serrated, tubercle, or adaptive propeller, as shown in Figure 2.2.

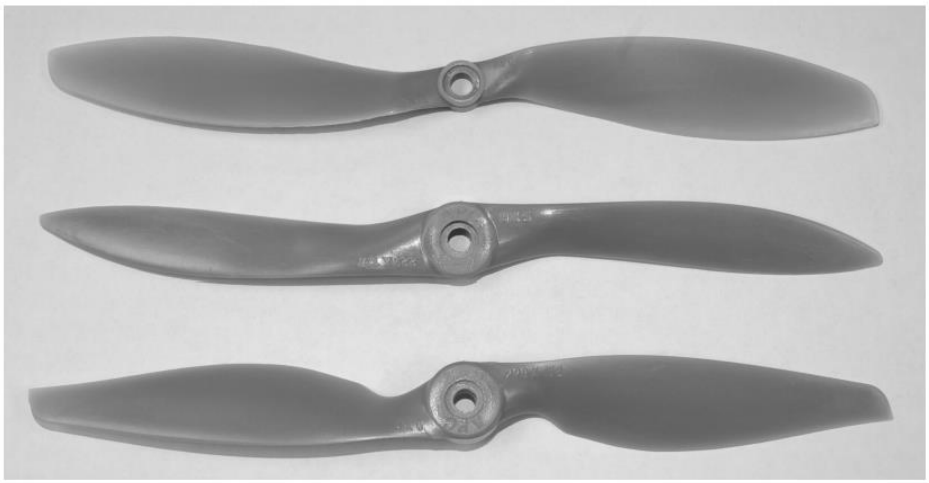

Figure 2.1: Conventional Propeller design of APC Slow Flyer (Brandt & Selig, 2011)

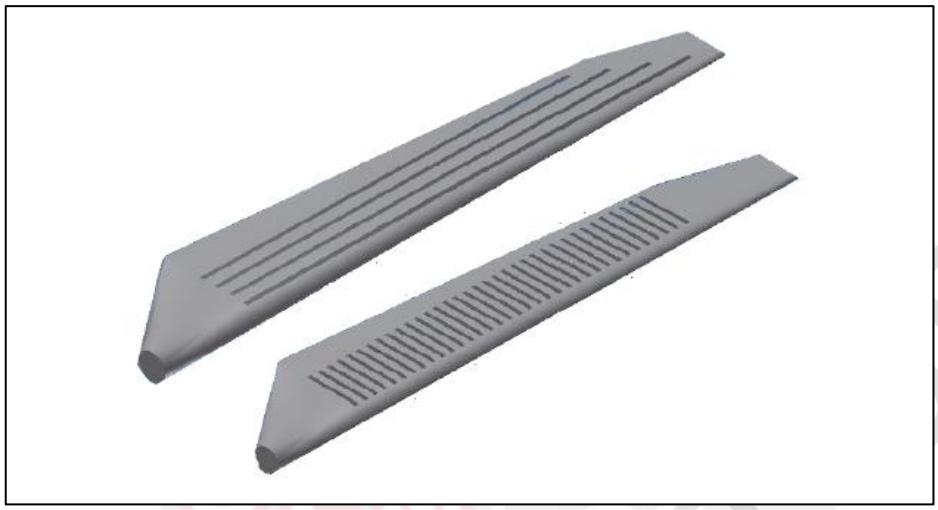

Figure 2.2: Unconventional design propeller of slotted propeller (Kutty & Rajendran, 2017)

From previous studies of propeller blade design, the conventional design of propeller received the main attention for design improvement. (Lee, 1998) conducted a study on propeller blade shape optimization for efficiency improvement. The study focused on the basic propeller design of a commercial aircraft propeller where the method of optimization can be used in any propeller blade design. The chord and twist angle was studied and the results showed that this optimization method is suitable for validating the designed propeller and selected as the great design tool for high-efficiency propellers.

(Kwon et al., 2012) performed a study on the enhancement of wind turbine aerodynamic performance using optimization of PARSEC method (Sobieczky, 1999). The authors used CFD for both 2D and 3D models to investigate the performance of the new design of wind turbines. The result showed that the design improved the baseline of wind turbine performance by 11%. (Sudarsono et. al, 2013) carried out the design optimization of airfoil propellers of modified NACA 4415 using CFD. The result showed that the modified NACA 4415 with different Reynolds numbers have better performance compared to the normal NACA 4415.

(Kwon et al., 2015) designed an efficient propeller by using variable-fidelity aerodynamic analysis and multilevel optimization. The authors designed a multi-level framework for the aerodynamic design of an electric UAV under cruise conditions by using Blade Element Momentum Theory (BEMT) (Goldstein, 1929) and Navier Stokes flow solver of CFD. The radius of the blade, twist angle, chord length, and type of aerofoil was examined to optimise the design of an efficient propeller. It is concluded that the new design stated to be 5.7% improvement from the previous design.
(Derakhshan et al, 2015) carried out the optimization study in improving the wind turbine by using artificial neural network and artificial bee colony method by (S. Derakhshan & Mostafavi, 2011). The authors optimized the twist angle, chord line, and also pitch angle and investigated the performance using the CFD approach, and tested with the wind

tunnel. For twist optimization, 3.3% average increment was obtained at all speeds. (Traub, 2016) designed and analysed the propeller by involving the effect of stalls using a simplified method based on vortex theory. The method used is to eliminate the need for iteration in determining the induced angle-of-attack and small-angle approximations. The blade angle was varied from 15 degrees to a stall angle of 40 degrees. The result concluded that the method of design used is the best tool to design the optimal blade.

From the reviews in terms of conventional propeller blade design, it can be concluded that most of the conventional design of propeller blades is pre-determined using the complex methods, while the analysis of further improved design is determined through CFD simulation. Hence, the performance analysis of the propeller blade is discussed in the next sub-section.

2.4 Evaluation of Propeller Performance

Every device or engine has the performance of evaluation. Performance can be denoted as the efficiency of the device. Higher efficiency leads to a better working device since the output value is higher than the input value. There are few methods to evaluate propeller performance. These methods can be categorised into two, which are experimental and numerical.

For the experimental method, the propeller is tested in a wind tunnel similar to wing testing. There are two types of experiments, known as static flow and advancing flow conditions. For static flow, the propeller is rotated with particular Rotation Per Minute (RPM) values where torque and thrust are measured. Meanwhile, for advancing flow condition test, the method is almost similar to the static test but the inlet velocity in the wind tunnel is introduced with fixed RPM values. The acquired results of thrust and torque are measured and thus the efficiency can be calculated with the following parameters. For numerical analysis, the propeller design is examined by using the CFD approach with a common Three Dimensional (3D) design model. The numerical prediction is solved by using Reynolds Average Navier Stokes (RANS) with different viscous models including one or more equations models. CFD method had a huge impact on propeller design and analysis. From the simulation, the value of torque and thrust is generated and the efficiency is obtained, similar to the experiment.

2.4.1 Experimental Method

In the experimental method, the review is organized according to the year to highlight the evolution trend of the propeller performance. (Merchant, 2005) carried out the experimental study of UAV propeller performance of a low Reynolds number. The study focused on 30 propellers at low speed with the open return wind tunnel that operated at 30000 to 300000 Reynolds number. The test was compared with the experiment study by (Asson & Dunnt, 1991) for validation purposes in terms of procedure, system accuracy, and data quality. The results showed a good agreement between current and

previous works and managed to provide reliable sets of data for low Reynolds number applications.

(Brandt & Selig, 2011) experimented with propeller performance at low Reynolds number UAV. The study used 79 propellers with the range of Reynolds number of 50000 to 100000 with details investigation compared to (Merchant, 2005). The tested propellers were range from 9 to 11 inches' in diameter with two-bladed, which is the standard of UAV propeller design. The wind tunnel used was also the open-return type with the turbulent intensity of 0.1% (Selig & McGranahan, 1995). The study used different RPM ranged between 1500 to 7500 to examine the Reynolds number effect of different speed with fixed RPM to sweep over a range of advance ratios until the propeller reached zero thrusts or windmill state. The efficiency varied at a peak of 0.65 for the good design propeller and 0.28 for the poor design propeller. This showed that some parameters may affect the propeller performance such as the diameter of the propeller, angle of twist, and Reynold number.

Figure 2.3: Photograph of experimental setup for (Brandt & Selig, 2011)

Later, the research was continued by (Deters et al., 2014). The authors focused on the small scale UAV propellers due to increment in drag and decrement in the lift of the airfoil with small Reynolds Number range between 40 000 to 500 000 as stated by (Selig & McGranahan, 1995). The study used 27 propellers with a range of 2.25 to 9 inches' diameter propellers together with the new four 3-D printed propellers. The 3-D printed propellers were tested due to the geometrical limitation compared to 27 propellers. The diameter of the 3-D printed propeller was varied. The experiment was conducted at the

same wind tunnel with static and advancing flow test. The data indicated that the Reynolds number was predicted for 27 propellers. In the case of the 3-D printed propellers at the same Reynolds number, the performance showed similar results even with different diameters value. With these results, the performance of the new propeller with different diameter can be predicted. The new 3-D printed propeller produced the same performance with the other 27 existence propellers which operated in the same range of Reynolds number.

(Van Treuren, 2015) performed the experimental study of the small-scale wind turbine under low Reynolds number condition due to limited development of wind turbine rotor, as stated by (Spera, 2009). The test was executed by using an S283 aerofoil at the open-circuit wind tunnel. The result later had been compared with XFOIL software (Drela, 1989) for 2D computational model and the database of the University of Illinois Urbana-Champaign. The XFOIL software has its limitation since it is unable to capture the aerodynamic characteristic of low Reynolds number under 100000. Due to this problem, it is more suitable to perform the experimental study to capture the aerodynamic characteristic. The results deduced that the wind tunnel method is the best method for gathering both lifts and drag data of the propeller blade.

(McCrink & Gregory, 2017) conducted the study on blade element momentum modeling for low Reynolds electric propulsion system. Since Blade Element Momentum (BEM) model is suitable for the full-scale propeller, a new model involved BEM, tip losses correction, Mach effect, Reynolds scaling, and 3D flow component was created. The performance predictions were estimated by using Advance Precision Composite (APC) propellers with three different advance pitch in one revolution of blade. The APC propellers were tested in the open return wind turbine. The data from the experiment supported the prediction of the proposed BEM model.

From the following years, the UAV propellers were tested inside the open return wind tunnel to validate the performance of the existing propeller. Then, the design of the propeller blade was optimised before the optimised model was tested by using wind tunnel testing. From the reviews, fewer studies focused on the design of the propeller and its improvement especially on the propeller blade design performance of UAV.

2.4.2 CFD Method

In mechanical engineering there are two tools that plays important roles in the industries. The first on is for structure which is Finite Element Analysis (FEA) and the second one is Computation Fluid Dynamics (CFD). Computers are utilised to conduct the computations necessary to simulate fluid free-stream flow and fluid interaction (liquids and gases) with surfaces specified by boundary conditions.

In aerospace sectors, CFD has important role to the industry. With CFD, engineers can calculate, velocity, force, thrust, drag, lift and even pressure by using Navier-Stokes

equations. These complex equations can be simplified and solved by using numerical method usually by using Euler equations. The first CFD tool was only used for two-dimensional method to simulate a flow of a cylinder in 1930s (Milne-Thomson, 2011) . Now with the advancement of technology and research CFD can be used in three-dimensional or even simulation with time manipulation. CFD nowadays is versatile. Some researcher are using CFD to model tsunami wave.

CFD has become a great tool to evaluate the performance of the propeller. In recent years, many studies conducted to design and analyse propeller performance. The following reviews are according to years to see the trend of CFD in the propeller design and analysis. In this section, all propeller blades of the different fields were examined due to fewer studies on the design and analysis of propeller blades using the CFD approach.

(Subhas et al., 2012) conducted the CFD of a marine propeller flow and cavitation, of INSEAN E779 propeller model. The model was generated by using CATIA V5R20 with specific dimensions and the blade angle. The domain of simulation was 4 times bigger than the diameter, while the length is 3 times bigger than the diameter, so that no recirculation occurred during the solving process (refer Figure 2.4). The mesh was generated by ICEM CFD with structural hexahedral mesh with the number of cells for the entire domain was 1.3 million. Fluent 6.3 was used to simulate the CFD. For non-cavitation flow, the steady flow with 6.22m/s velocity inlet and outflow with the standard k-epsilon viscous model was used. SIMPLE, Standard pressure, and Quadratic Upwind (QUICK) discretisation methods were set up for the simulation. For cavitation flow, the same viscous model was used and the Multiple Reference Frame (MRF) was assigned to rotate the propeller with the rotational speed of 1500 RPM, 1800RPM, 2400RPM, and 3000RPM. The data of thrust and torque coefficient was obtained and compared with theoretical and experimental results of (Ianniello & National, 2015). The minimum and maximum difference values of both thrust and toque coefficients were 0.013 and 0.001, respectively.

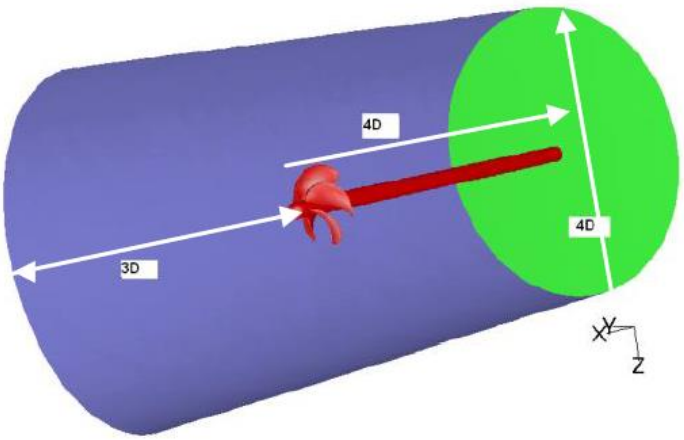

Figure 2.4: Domain of propeller full simulation of (Subhas et al., 2012)

(Kwon et al., 2012) studied the enhancement of horizontal wind turbine aerodynamic performance by using a numerical optimization technique. A new modified airfoil contour, known as the PARSEC shape function was used to achieve maximum lift-to-drag ratio for each blade station. By using CFD to validate the current S809 airfoil section in the 2D simulation with NREL experimental data (Somers, 1997). Hybrid mesh with 88790 number of cells was used where the structure mesh was obtained for capturing boundary layers of the airfoil and the unstructured mesh was obtained at the boundary region due to the complicated shape of the airfoil. Later, the new optimized aerofoil was selected at NREL Phase IV rotor blade considering twist angle and chord length distribution. The steady flow was used in this 2D airfoil and 3D propeller simulation with transition turbulence model for the 2D simulation and SST turbulence model for 3D simulation. The results showed that 11% improvement of torque and 8% improvement of thrust was acquired.

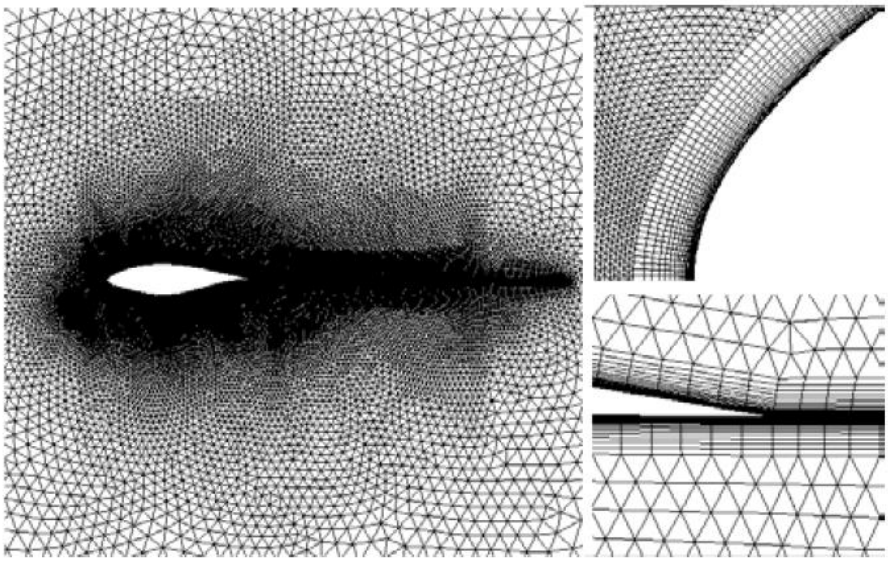

Figure 2.5: Two-Dimensional mesh of S809 of (Kwon et al., 2012)

(Sudarsono et al., 2013) conducted the design optimization of the airfoil propeller for the horizontal wind turbine of the modified NACA 4415 using CFD. In the study, NACA 4415 was set as the base design, and the optimised design is known as NACA 4415 modified. The blade was constructed by CAD software and computational modeling was done on ANSYS FLUENT 12.1. Spalart-Allmaras turbulence model was utilized during the simulation considering the steady-state condition and only the coefficient of lift and drag was obtained. The results showed that NACA 4415 modified has a better performance compared to NACA 4415 at Reynolds number of 4.1×10^4 and 2.5×10^5 where the drag of NACA 4415 is higher compared to NACA 4415 modified model.

(Morgado et al., 2015) designed and analysed the high altitude propeller for Multibody Advanced Airship for Transport (MAAT) cruiser. To obtain an optimised propeller, the inverse design methodology based on minimum induced losses was used in the JBLADE

software (Silvestre et al., 2013). Two different blades designed were conducted; namely the best L/D and the best $L^{3/2}/D$. Both propellers had fixed hub and diameter. The mesh was generated with 2.7 million tetrahedral cells. ANSYS FLUENT was used to simulate the problem by using Multiple Reference Frame (MRF) with angular velocity of 100 to 550 RPM that increased gradually. Inlet velocity was also introduced which range from 10 ms^{-1} to 65 ms^{-1}. K-omega SST turbulence model was used to solve this simulation. The authors found that the design of $L^{3/2}/D$ produced bigger pressure difference between upper and lower surfaces compared to L/D blade. Hence, the authors proven that $L^{3/2}/D$ have more thrust compared to L/D blade which is then selected as the propeller of MAAT cruiser.

(Stajuda et al., 2016) performed the CFD model for the propeller simulation. The authors investigated the difference between disk thickness for MRF for the single propeller and also highlighted the meshing approach and numerical setup. The propeller used in this study was the Vertical Take-Off and Landing (VTOL) aircraft propeller from a previous study by (Karczewski & Eglin, 2014). The propeller used was the available market propeller to compare the propeller performance between CFD and experiment. ANSYS CFX solver software was used in this study with MRF of 0.84 to 1.16 nominal speed for the propeller to rotate., while the mesh for propeller was generated using ICEM CFD. Hybrid mesh with structured hexahedral on the propeller and rotating domain and unstructured tetrahedral mesh on the stationary domain were considered with 3 million number of cells. Shear Stress Transport turbulence model was used in the simulation and the results showed that the simulation of the propeller agreed with the result of the experimental. The authors also found that higher velocity or rotational speed, lead to bigger disc size needed for MRF in order to capture the fluid flow behaviour.

(Nouri & Mohammadi, 2016) conducted the study on the performance of NACA marine propellers by increasing the number of propellers with the aid of CFD. 4-digit NACA airfoil was used in the study and few numbers of blades were introduced on the propeller. The number of blades ranged from 3 blades to 15 blades. The authors used ANSYS CFX to solve numerical prediction. The simulation used hexahedral mesh in all zones except for small cylinders around the propeller where the tetrahedral mesh was selected due to the complicated shape of the propeller. In this simulation, MRF was used with different inlet velocities. The K-epsilon RNG turbulence model was used for this simulation. Validation with previous experiment data from (Barnitsas et al., 2012) showed that the best number of the propeller for NACA marine propeller is 9. As the number of blades exceeding 9, the performance of the propeller decreased.

(Kuantama & Tarca, 2017) determined the performance of ducted propeller for UAV design, as shown in Figure 2.6. The authors hypothesized that the disturbance effect decreased and the thrust of the propeller increased as the propeller added with ducted design (Hrishikeshavan et al., 2012). The authors performed a CFD analysis of propeller with a non-ducted propeller, and different type of ducted propeller. The results indicated that ducted propeller improved the performance of propeller with limited duct size with 2.1 N of thrust. This is because the duct with a bigger size influenced the increment weight of the drone, and hence UAV flight performance may be affected. The study

showed that the propeller type ß with bigger duct size showed small improvement performance compared to type α and γ.

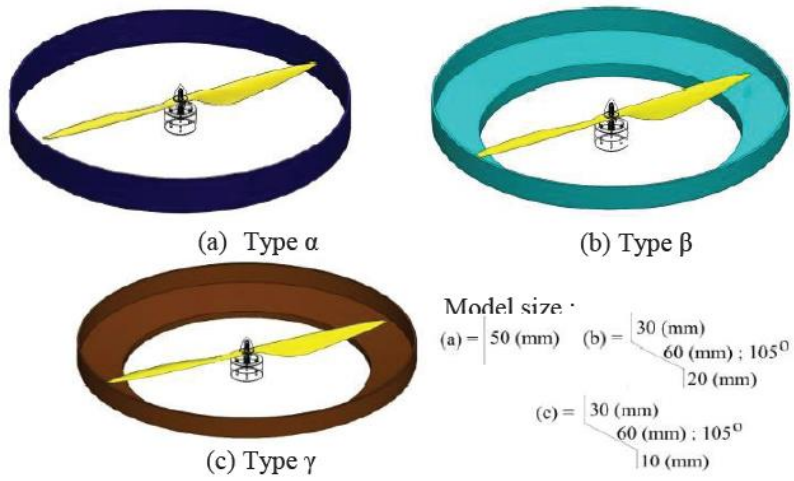

Figure 2.6: The example of ducted propeller model for (Kuantama & Tarca, 2017)

(Han et al., 2017) carried out the experimental and computational analysis of microscale shrouded coaxial rotor in hover state. The coaxial rotor is referred to as a rotor with two propellers that are placed diagonally. The authors compared the coaxial rotor and also shrouded coaxial rotor which was the ducted coaxial rotor. The coaxial rotor produced a huge advantage for the microscale rotor since the diameter of a single rotor reduced and the same amount of net thrust with the same blade and disk load produced (Fernandes, 2017). The blade pitch angle of propellers, the rotor spacing, and tip clearance was studied in both experimental and numerical. The authors used ANSYS FLUENT to simulate the study with MRF at the rotating zone with a rotational speed of 1000 to 7000 RPM. The mesh was generated by using ICEM CFD with structured hexahedral mesh. Spalart-Allmaras turbulence model was considered in this study to solve the analysis. The results concluded that the coaxial rotor was suitable for smaller pitch angle condition while the shrouded coaxial rotor was suitable for larger pitch angle condition.

(Ben Nasr et al., 2017) studied the aircraft propeller analysis using Blade Element Momentum Theory (BEMT) and CFD. The study was about theory and numerical analysis of aircraft ONERA, NLR, and MT-propeller. The author used ElsA (Cambier et al., 2013) and ENSOLV (Brouwer, 1992) CFD solver that used the rotational motion of 1500 RPM to 1700 RPM. The mesh generated was hexahedral mesh with 5 million number of cells. K-omega KOK and Wilcox models were used in this simulation to solve the numerical prediction. This study allowed reviewing the methods and tools between partners to launch the design and optimization activities with good confidence concerning the obtained performance.

(Yoon et al., 2017) conducted the computational aerodynamic modeling of small quadcopter vehicles. In this study, the researcher compared the placement of the propeller blade of the UAV body. The propeller was placed over the UAV body, under the UAV body, and off-body of the UAV, as shown in Figure 2.7. The authors used OVERFLOW (Pulliam, 2011) to solve the simulation with the rotational speed of the propeller blade of 5400 RPM. In order to mesh the model of UAV and propeller, the author used CHIMERA grid tools (Chan, 2002), where the software able to performed mesh for the complex shape with structured grid mesh. Spallart-Allmaras turbulence model was used to solve the numerical equations of RANS. The results showed that the under-mount rotors generated higher thrust compared to off-body under-mount. However, the best place to locate the rotor for UAV was still overmount where the rotor was placed above the UAV. High-fidelity CFD can be effectively used to examine design parameters and thereby to help in improving the design of next-generation multi-rotor drones.

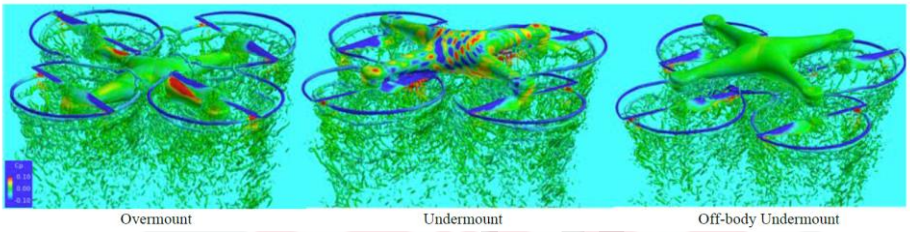

Figure 2.7: The placement of propeller (overmount, under-mount and off-body under-mount) at the body of the UAV (Yoon et al., 2017)

(Anemaat et al., 2017) conducted the study on aerodynamic design, analysis, and testing of propellers for small UAV. The authors used Blade Element Momentum Theory (BEMT) (Drzewiecki, 1920) (Stepniewski & Keys, 1984) and CFD to analyse the propeller design. The authors stated that the available propeller was not designed properly. The propeller was designed by DAR corporation where the chord and pitch distributions were based on Navy 5868-9 propeller. STAR-CCM+ was used to solve this simulation with the rotation of 10000 RPM with freestream velocity. The mesh was generated polyhedral with the shape of many polygons usually pentagon. The results showed that the propeller produced by DAR corporation improved in performance compared to OEM propellers that usually have no angle or twist. The torque, thrust, and efficiency characteristics as the function of propeller advance ratio were captured throughout the study.

(Yomchinda, 2018) performed the CFD simulations of the wake or airflow velocity from the commercially-available propeller of the 3-D scan model and the virtual model in a hovering condition were investigated. The authors insisted to understand the flow wake behavior of the propeller since there were fewer studies related to the wake flow of the propeller. To solve the simulation, ANSYS FLUENT was used with MRF at the rotating domain at different rotational speeds, known as 5000RPM, 6000RPM, and 7000RPM. The results showed that 10% to 29% error was measured in thrust computations from the static test result. The comparison results showed the feasibility of using a virtual model to represent the actual propeller model in the generation of wake in CFD computations.

The future work of the propeller in different operating conditions will be further investigated.

(Yang et al., 2018) studied the effect of blade pitch angle on the aerodynamic characteristic of the straight-bladed vertical axis wind turbine for experimentally and numerically approaches. The authors investigated the effect of different pitch angle of NACA0021 with two blades vertical axis wind turbine. In order to understand the performance of the wind turbine, the simulation was solved by using ANSYS FLUENT. Sliding mesh method was used, as shown on Figure 2.8, hence the input velocity able to move the propeller blade as compared to MRF method, where the blade was rotate by a rotor. Hexahedral mesh was used at the 2D simulation of the propeller blade. The author used K-omega SST turbulence model to solve the simulation. Validation was made with previous experiment data by Yang et al. (Yang et al., 2017) The results showed that the blade pitch angle affected the pressure distribution on the single blade surface and the torque coefficient also affected the blade pitch angle. On top of that, certain blade pitch angles improved both torque and power of the wind turbine. For example, pitch angle of $6^{o,}$ performed the maximum pressure difference on the blade surface, while8^{o} blade pitch angle showed maximum pressure coefficient on the downstream region.

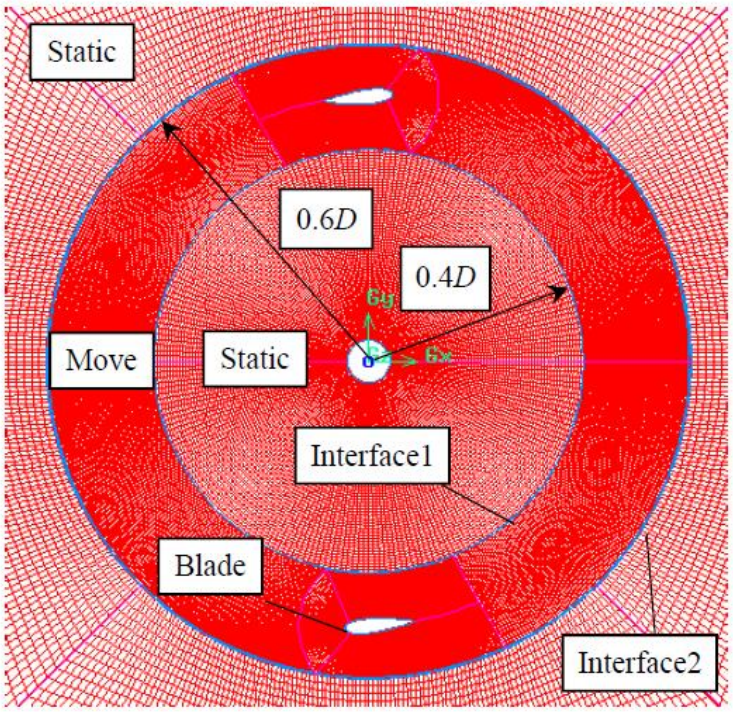

Figure 2.8: Rotating region mesh of MRF of (Yang et al., 2018)

(Andrés et al., 2019) performed the computational study of a small rotor of hover using CFD approach and Unsteady Vortex Lattice Method (UVLM), which commonly used on

the helicopter by (Colmenares et al., 2015). The authors selected the UVLM as the model to design the small rotor propeller compared to other studies which mostly used the BEMT approach. ANSYS FLUENT 17 was used to solve the simulation with MRF at 1RPM to 4500RPM. Unstructured tetrahedral mesh with a refined layer of pyramidal elements was applied near the rotor surface. The authors also used K-omega SST for the turbulence model selection of the simulation. The results showed that the difference in the prediction of thrust coefficient between computational methods and experimental data is less than 9%. Both methods overestimated the thrust by 3% and 12% for CFD and UVLM respectively, with respect to the flight test results.

(Eltayesh et al., 2019) studied the effect of wind tunnel blockage on the performance of a horizontal axis wind turbine with a different number of blades. The authors examined the role of wind tunnel blockage on a small size wind turbine with a different number of propeller blades of three and five blades. The authors used ANSYS FLUENT to solve the simulation with different velocity inlets and different rotational speeds by using the MRF technique. The mesh was generated using ICEM CFD with 4.3 to 4.8 million cells for 3 and 5 blade models, respectively. K-omega SST was used to solve the numerical prediction and the result showed that the higher number of blades produced a higher performance of the wind turbine.

(A. Amiri et al., 2019) performed the study on horizontal axis tidal turbine performance and investigated the best pitch angle using CFD. The authors used the three-bladed rotor that was designed using Computer Aided Drawing (CAD). Five-digit NACA airfoil was used to design the propeller blade with a diameter propeller of 470mm. The pitch angle varied from 0 to 30.5 degrees. ANSYS FLUENT with MRF at the rotational domain with 70RPM was used to solve the case. Two free stream velocity was introduced at the velocity inlet. The unstructured mesh was generated with relevant Y+ with 3.88 million number of cells. K-epsilon turbulence model was used to solve the numerical solution. The validation process was carried out using AeroDyn BEM code. The result showed that the highest power is at 19.3-degree pitch angle.

(Stan, 2019) designed the marine propeller blade with jet holes and a backflow screen. The authors stated that this designed propeller lead to an increase in performance of the marine propeller due to the whirlpool generated by the propeller design. In this study, ANSYS FLUENT was used as the CFD software. with the boundary condition of steady flow and inlet velocity of 28.87m/s to mimic the rotational motion of the blade. The velocity inlet was placed at the side of the propeller, while the outlet was placed at the back of the propeller. The model was meshed with 191033 number of cells. K-epsilon as the turbulence model. The results showed an improvement in the propeller performance by changing the features of the propeller. Further experiment data needed to be analysed to validate the result of numerical data.

(Ali et al., 2019) analysed the propeller design for the medium-sized drone. The DJI Phantom 3 drone was selected to be used in this study as a commercially available drone. Three types of propellers were used in this project, namely normal, bullhorn, and hybrid bullhorn propeller. The authors used ANSYS FLUENT solver for the simulation case with MRF at the rotating domain of 800 RPM. The unstructured mesh was used,

however, the mesh data was not stated in the study. K-epsilon turbulence model was used to solve the numerical simulation. The normal propeller was selected as the best propeller in this study because it produced a high lift coefficient with a low drag coefficient compared to the others.

(Malmir, 2019) carried out the CFD simulation of skew angle and blade number of a marine propeller. The marine propeller blade was designed by using CAD and the author varied the skew angle of the propeller blade and also the number of the blade, as shown in Figure 2.9. The skew angles were varied from 0°, 13°, 26°, and 52°. ANSYS FLUENT was utilized to solve the numerical method. The unstructured mesh was used in this simulation with 2 million cells. K-omega SST was selected for the viscous model. The result concluded that the increment of the blade number has a positive impact on the propeller performance. Meanwhile, for skew angle, higher skew angle resolved in low performance.

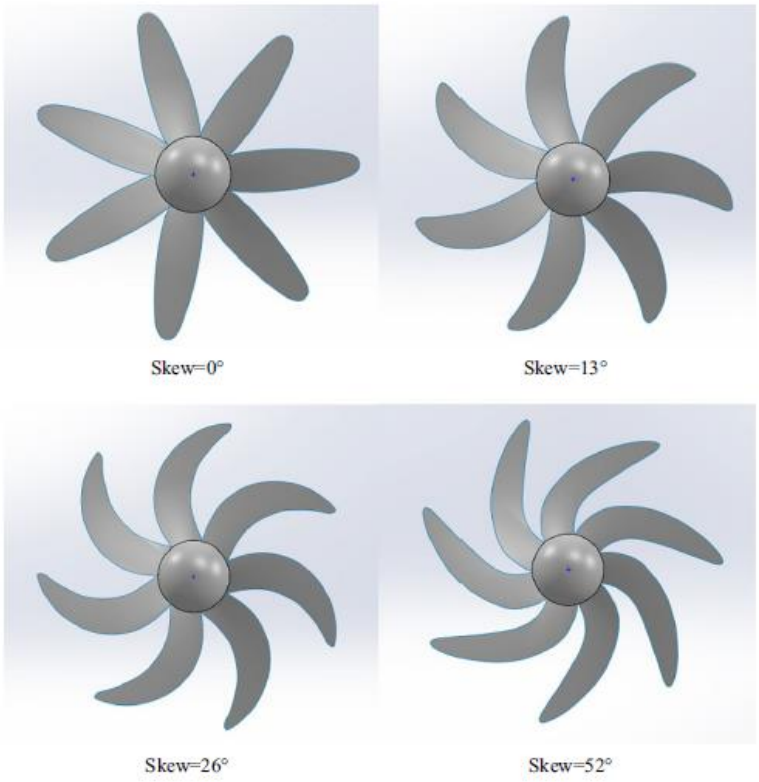

Figure 2.9: Skew angle configuration of (Malmir, 2019)

(Kutty & Rajendran, 2017a) studied on the 3D CFD simulation and experimental validation of small APC Slow Flyer Propeller Blade known as commercialising propeller. The authors compared the result of propeller efficiency with the CFD results by (Brandt & Selig, 2011) and (Deters et al., 2014) which experimented with determining

the propeller performance. The authors used unstructured meshing with different turbulence models, which are k-ϵ and k-ω and compared to the difference and error of the blade efficiency. As a result, the k-ω showed a more accurate result compared to other turbulence models.

2.5 Literature Finding

From the reviews studied, several findings are highlighted. In terms of the design of the propeller, fewer studies focused on the propeller design of the UAV propeller. There are many validations are made by using CFD. Table 2.1, shows the current study that used CFD as a tool to study the propeller.

Table 2.1: Study of propeller performance using CFD

Author	Type of propeller	Study
(Subhas et al., 2012)	Marine	Propeller and Cavitation effect on marine propeller
(Kwon et al., 2012)	Wind Turbine	Aerofoil Shape
(Sudarsono et al., 2013)	Wind Turbine	Aerofoil Shape
(Morgado et al., 2015)	UAV	Performance on High Altitude Propeller
(Stajuda et al., 2016)	Helicopter	Disk Thickness, meshing approach and Numerical Setup
(Nouri & Mohammadi, 2016)	Marine	Number of blade
(Kuantama & Tarca, 2017)	UAV	Ducted propeller study

Table 2.1: Continued

(Han et al., 2017)	UAV	Coaxial rotor
(Ben Nasr et al., 2017)	Helicopter	Study on new CFD solver
(Yoon et al., 2017)	UAV	Placement of propeller on UAV
(Anemaat et al., 2017)	UAV	3D scan and improved market design propeller
(Yomchinda, 2018)	UAV	3D scan and static test propeller
(Yang et al., 2018)	Wind Turbine	Effect of pitch angle
(Andrés et al., 2019)	UAV	Wake of propeller
(Eltayesh et al., 2019)	Wind Turbine	Number of blade
(A. Amiri et al., 2019)	Tidal Turbine	Number of blade and pitch angle
(Stan, 2019)	Marine	Jet holes on propeller
(Ali et al., 2019)	UAV	The type of hub of propeller
(Malmir, 2019)	Marine	Skew angle and number or blade

Table 2.1: Continued

(Peng et al., 2019)	Marine	Size of MRF

Referring to Table 2.1, fewer studies focused on designing UAV propellers. There are several studies focused on the design of wind turbine and large scale propeller. Meanwhile, several studies investigated the large-scale propeller and marine propeller which operated at a high Reynolds number which is different than the low scale propeller since it operated at a low Reynolds number.

CFD is a great tool to evaluate the performance of the propellers. The trends show that, as time-evolving, CFD is used as the tool for evaluating propeller performance. MRF is a great function in the CFD so that the propeller CAD model can be rotated as the propeller rotating on the motor. In terms of meshing, both structured and unstructured meshes provide a good result proven from the validations by previous studies. The structured mesh was used for the uncomplicated geometry of the propeller, while the unstructured mesh was used for a complicated geometry. For example, a propeller with high skewness required a design with complicated twists.

ANSYS FLUENT also the most popular software employed to solve the numerical prediction. This is because ANSYS FLUENT is available in the market and it is user friendly. The user interface is easy to use and MRF also can be accessed easily. Only four equations of viscous model became the most applied, which is k-epsilon and k-omega because both viscous models provided high accuracy results compared to 2 equations model like Spallart-Allmaras.

In terms of design, studies mostly available highlighted chord, twist angle, aerofoil, blade numbers, blade diameter, blade thickness, and pitch angle. Propeller is made up of many airfoils with different chord sizes and pitch angles that are enclosed together. However, no study available that discussed the blade position of origin. This topic needs to be discussed because it is very important during designing the APC Slow Flyer Blade with the position of the origin of the airfoil, which is not stated in the geometrical data by (Brandt & Selig, 2011). This is the reason for this study is essential to be discussed. Further study needed to be performed, so that the design of low Reynolds number propeller can be developed properly.

2.6 Summary

This chapter discussed the evolution of the propeller blade in terms of working principle and evaluation performance. Implementing propeller blade design has proven its improvement on airfoil shape, chord length, angle twist, and blade angle of attack through various optimisation methods. To date, there are insufficient reviews on the blade

position of origin provides a comprehensive understanding of this topic. Hence, experiment and CFD analysis has proven to be the best method to determine the performance of the propeller blade design. Here, studying the blade position of origin have become the objective of the study. Understanding the effect of the parameter may give significant advantage or disadvantage. This study main purpose is to understand the effect of blade position of origin to the aerodynamic performance of the propeller.

CHAPTER 3

METHODOLOGY

3.1 Introduction

In previous chapter, the objective of the study was mentioned. There is an interesting parameter that can be study. In this chapter, thorough process will be explained on how the study is conducted. The first part of the chapter is on the flow chart of the process of the study. The flow chart is presented so that it will be a layout on how the chapter will be explained.

The second part of the chapter is on how the simulation is modelled. Since this study mainly focus on Computational Fluid Dynamics (CFD), thorough process on CFD will be explained. CFD have three main process. The first part is pre-process, second one is solving the CFD equation or model and third is post process which involve in analysing the qualitative data and quantitative data.

For the pre-process, modelling the propeller and domain is the most important thing. After that, grid was generated on the model since CFD use the method of finite element method to solve the equation. The boundary condition, turbulence model and solver is chosen in order to solve the analysis.

For the solver, type of software and solver is chosen wisely in order to obtain the reliable data. Mesh dependency, turbulence dependency and validation is carried out so that the data is reliable.

For the post process, there are two types of data that can be discussed. Quantitative data is the difference and error between the previous and present study. Qualitative data is more on the pressure gradient since that is what interest the most in CFD.

3.2 Project Flow Chart

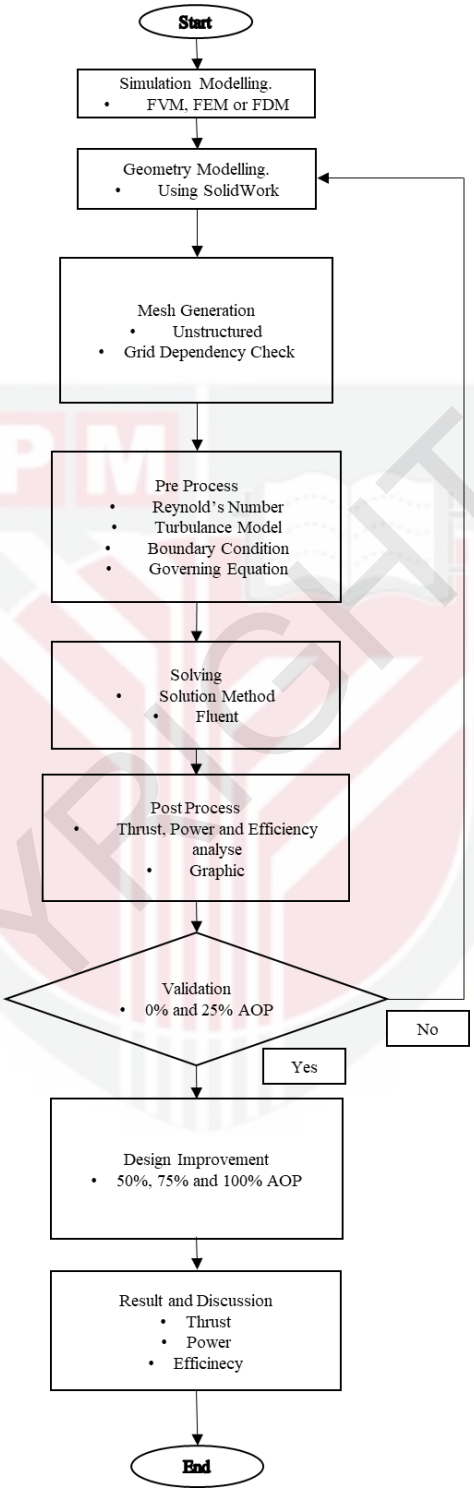

Figure 3.1: Project Flow Chart

3.3 Simulation Modelling

Before the analysis will be carried out. A proper simulation modelling need to be carried out so that our analysis is sure right one. CFD can be solve using three types of method which are Finite Difference Method (FDM), Finite Element Method (FEM) and Finite Volume Method (FVM).

FDM is a method that is easy to program. It is based upon the differential form of the PDE to be solved. Each derivative is replaced by a formula that approximates the difference (that can generally be derived from a Taylor series expansion). The solution is obtained at each nodal point, and the computational domain is commonly divided into hexahedral cells mesh. The FDM is easiest to understand when the physical grid is Cartesian, but it can be extended to domains that are not easily represented by brick-shaped elements by using curvilinear transforms. The discretization produces a system of equations at nodal points for the variable, and once a solution is found, we have a discrete representation of the solution. Unfortunately for this study, due to the complex geometry of the propeller FDM is not an option.

There are 2 other methods that can be used which are FEM and FVM. Usually FEM is used in structural analysis of solid, but it also applicable for fluid analysis. A discretization using the finite element method (FEM) is based on a piecewise representation of the solution in terms of specified basis functions. The computational domain is subdivided into smaller domains (finite elements), and the solution in each element is built using the basic functions. The actual equations are usually obtained by restating the conservation equation in weak form: the field variables are written in terms of the basic functions, the equation is multiplied by appropriate test functions, and then integrated over an element. Because the FEM solution is expressed in terms of specific basis functions, it is much more well-known than the FDM or FVM solutions. This can be a double-edged sword because the selection of basic functions is critical, and boundary conditions may be more difficult to formulate. Again, a system of equations (usually for nodal values) is obtained that must be solved in order to obtain a solution. The FEM require more memory and time to solve compare to FVM according to (Molina-Aiz et al., 2010).

The discretization of a finite volume method (FVM) is based on an integral form of the PDE to be solved (e.g. conservation of mass, momentum, or energy or Navier-Stokes Equation). The PDE is written in a way that it can be solved for a finite volume (or cell). The computational domain is discretized into finite volumes, and the governing equations are solved for each volume. The resulting system of equations usually includes fluxes of the conserved variable, so flux calculation is critical in FVM. The primary advantage of this method over FDM is that it does not require the use of structured grids, and the effort required to internally convert the given mesh to a structured numerical grid is completely avoided. The finite volume equation yields governing equations in the form,

$$\frac{\partial}{\partial t}\iiint Q\,dV + \iint F\,d\mathbf{A} = 0,$$

where Q is the vector of conserved variables, F is the vector of fluxes (such as Euler equations or Navier–Stokes equations), V is the volume of the control volume element, and A is the surface area of the control volume element. Due to the advantage in memory usage and solution speed, especially for large problems, high Reynolds number turbulent flows, and source term dominated flows (like combustion) FVM is used for this analysis. The CFD software that utilized FVM is ANSYS Fluent.

Since this analysis is a propeller analysis, the propeller need to be rotating with respect rotation per minute. Multiple Reference Frame (MRF) was utilized because there will be two zones that interacting in this analysis. The propeller can be rotate with respect to the rotational speed and there will be inlet velocity which is a static domain. Because previous study from (Kutty & Rajendran, 2017a) had used this method, this analysis will used the same method using ANSYS Fluent with MRF.

3.4 Propeller Model

The propeller models were created using the experimental data obtained from (Brandt & Selig, 2011). The propellers were modelled using SolidWorks. The APC Slow Flyer is a two-bladed propeller with a hub in the centre. It is a fixed-pitch blade with a diameter of 0.254 m. The propeller consists of two types of the airfoil which are, Eppler E63 and Clark-Y airfoil near the tip according to (*Engineering | APC Propellers*, n.d.). The profile of the blade is shown in Table 3.1. Based on the data provided, there are 19 stations of the airfoil to produce a blade.

Table 3.1: The propeller geometry data retrieved from UIUC

r/R	R (mm)	c/R	c (mm)	Beta (°)
0.15	19.05	0.109	13.843	34.86
0.20	25.40	0.132	16.764	37.60
0.25	31.75	0.155	19.685	36.15
0.30	38.10	0.175	22.225	33.87
0.35	44.45	0.192	24.384	31.25
0.40	50.80	0.206	26.162	28.48

Table 3.1: Continued

0.45	57.15	0.216	27.432	25.60
0.50	63.50	0.222	28.194	22.79
0.55	69.85	0.225	28.575	20.49
0.60	76.20	0.224	28.448	18.70
0.65	82.55	0.219	27.813	17.14
0.70	88.90	0.210	26.670	15.64
0.75	95.25	0.197	25.019	14.38
0.80	101.60	0.180	22.860	13.11
0.85	107.95	0.159	20.193	11.83
0.90	114.30	0.133	16.891	10.65
0.95	120.65	0.092	11.684	9.530
1.00	127.00	0.049	6.2230	8.430

The radius of the blade is 0.127 m and the radius of each station of the airfoil is calculated and the blade is constructed using SolidWorks. Each station is presented on a plane that contain the section of the airfoil. Lofted boss base feature was used so that a solid model of propeller can be generated.

The blade was constructed with five different AOP percentages which were 0%, 25%, 50%, 75% and 100%. Figure 3.1 shows the representation of airfoil with different positions of origin where the original location can be referred to as highlighted with red colour. The design of the propeller was based on an Eppler 63 airfoil at one station as indicated by the red curve. The black horizontal line (highlighted with red colour) represents the centre of the hub. As the black horizontal line located at the leading edge of the airfoil, the blade was shifted forward and downward. In contrast, as the black horizontal line located at the trailing edge of the airfoil, the blade was shifted backwards and upward.

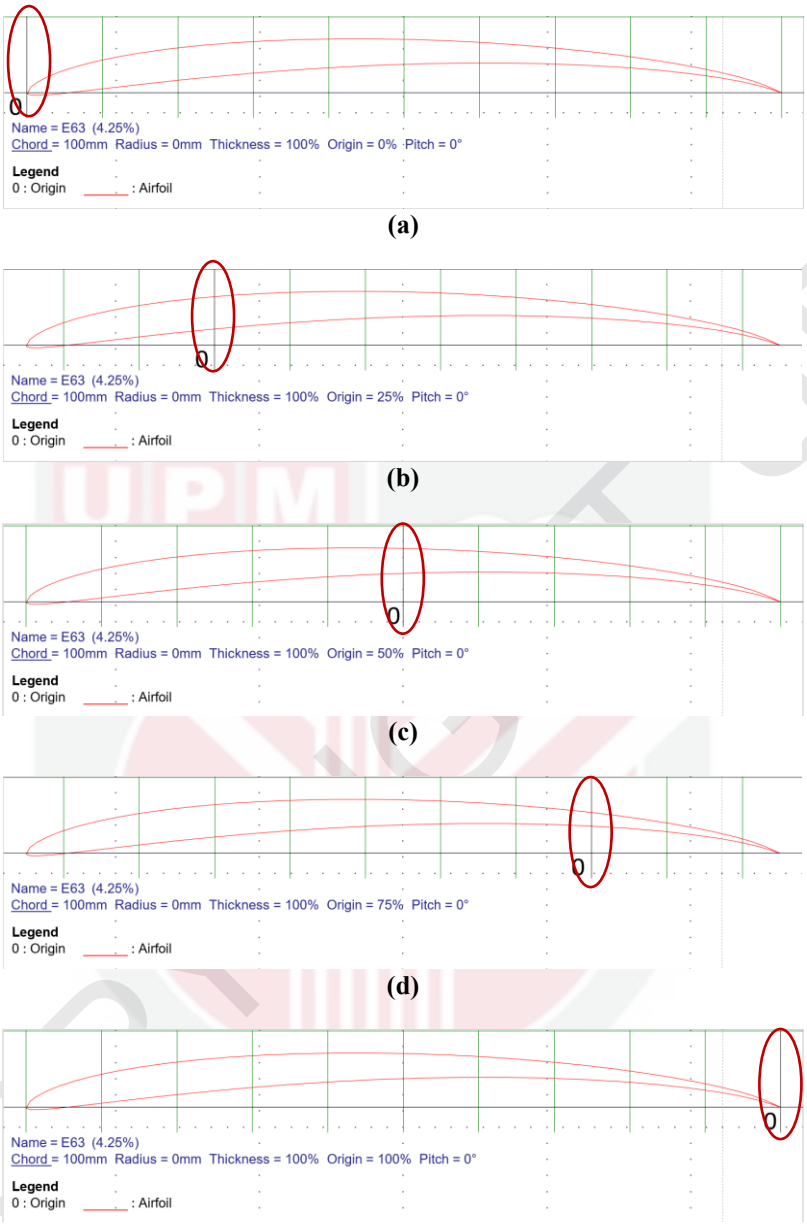

Figure 3.2: E63 airfoil at 100mm length with (a) 0% AOP (b) 25% AOP (c) 50% AOP (d) 75% AOP (e) 100% AOP

The huge impact of changing the percentage of AOP can be observed when designing the twist blade design. The existence of 19 stations of the airfoil with different chord length value and airfoil angle of attack influenced the twist of blade design (refer Figure 3.2 a and b). Figure 3.2 (a) represent the distance airfoil station with a different chord length of airfoil. Meanwhile, Figure 3.2 (b) shows a better perspective of the relationship

between the stations' distance, position of airfoil origin, chord length and angle of attack which lead to the development of the different shape of twist blade design.

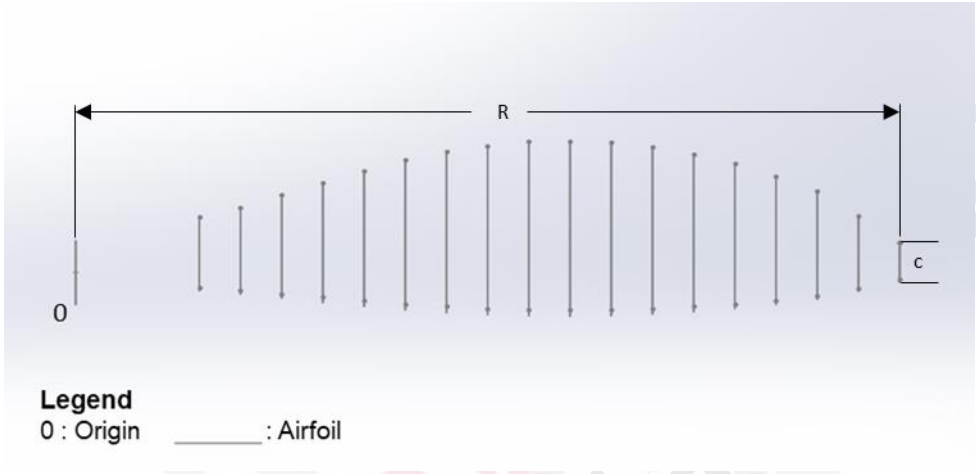

(a)

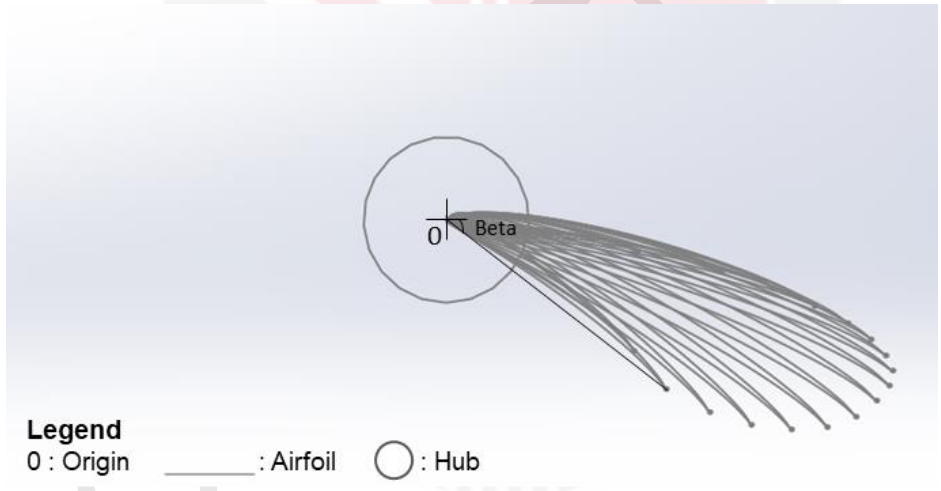

(b)

Figure 3.3: (a) The airfoil geometry at each station top view (b) The airfoil geometry at each station side view

The blade was constructed with five different positions of origin. In this study, the five positions of origin analysed were categorised as 0% AOP, 25% AOP, 50% AOP, 75% AOP, and 100% AOP. This relationship has led to the development of different shapes of the propeller blade design. By changing positions of origin at each station, it has changed the aerodynamics shape of the propeller design due to the effect of different twist angle of each station. Figure 3.3 shows the different positions of origin of the same basic design

of APC Slow Flyer and depicts the side view of the APC Slow flyer with different positions of origin.

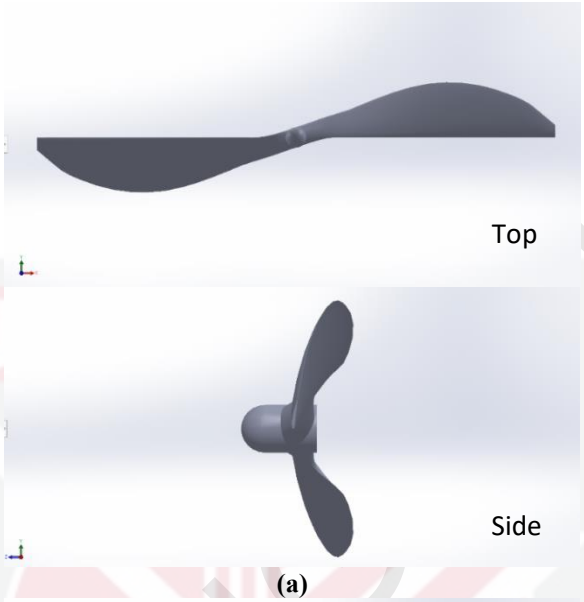

(a)

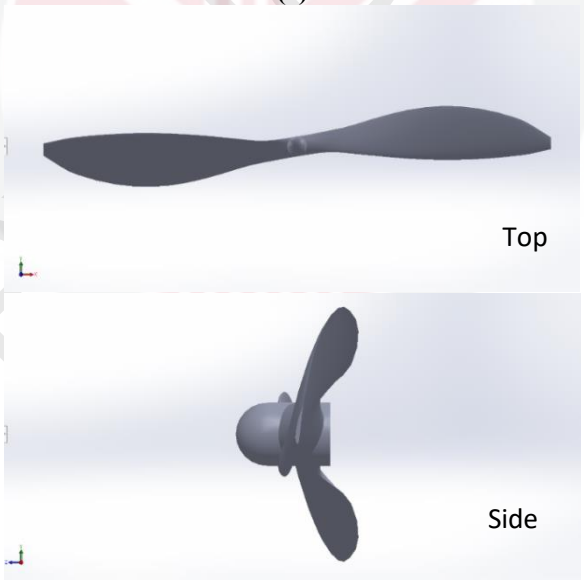

(b)

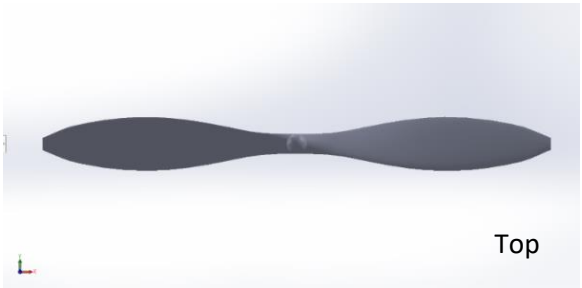

(c)

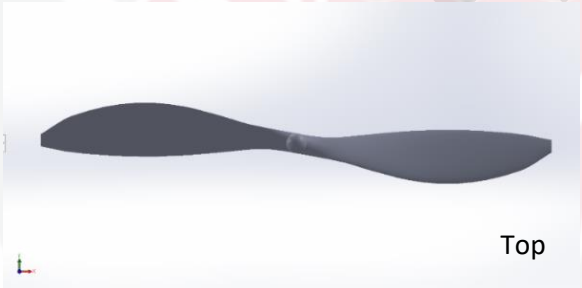

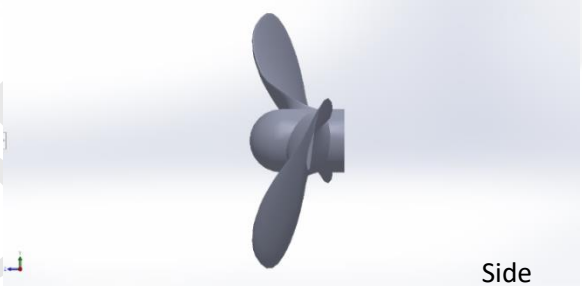

(d)

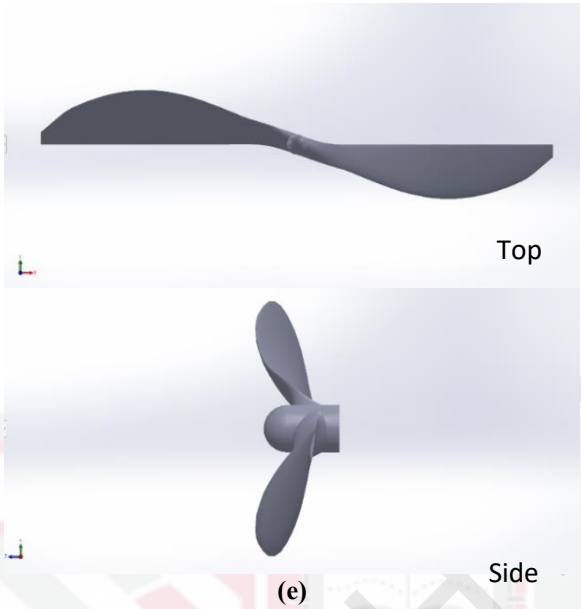

Figure 3.4: APC Slow Flyer top and side view with (a) 0% AOP (b) 25% AOP (c) 50% AOP (d) 75% AOP (e) 100% AOP.

3.5 Flow domain

The flow domain was constructed using SolidWorks as a similar development concept by (Kutty & Rajendran, 2017a). Figure 3.4 shows the domain, rotating domain, velocity inlet, and outlet and Figure 3.5 is the schematic diagram of the simulation.

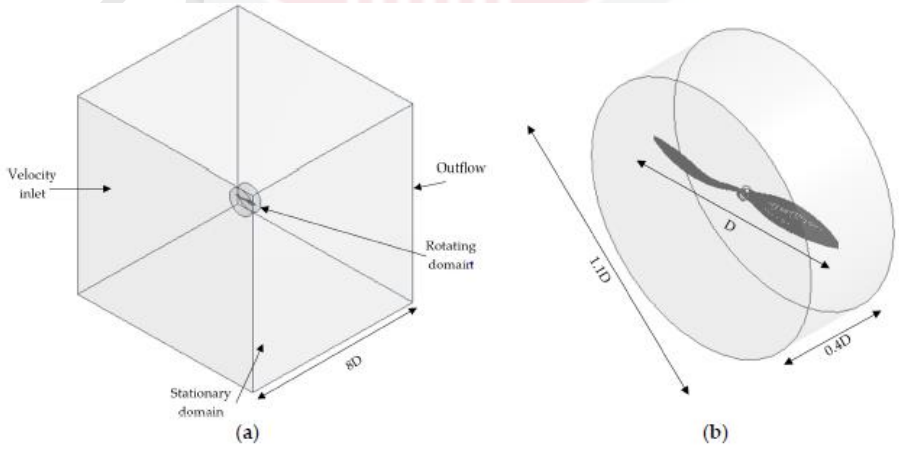

Figure 3.5: The domain of the simulation a) the stationary domain b) rotating domain (Kutty & Rajendran, 2017a)

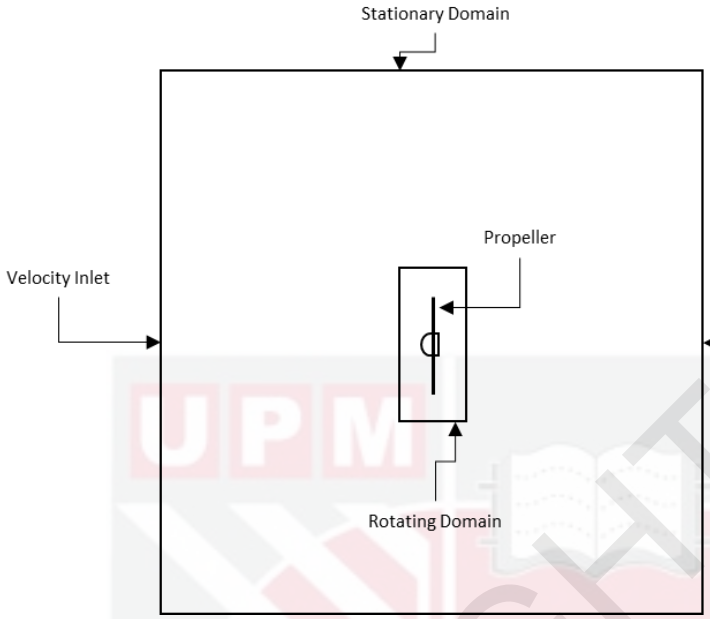

Figure 3.6: Schematic diagram of the analysis

The numerical predictions were performed using Fluent 18.2 released by ANSYS, Inc., Canonsburg, PA, USA, a commercial CFD solver. The flow of the blade was simulated using the MRF model on the rotating domain. The domain was defined as stated in Figure 3.4. The domain was split into two, which were the rotating domain and the global stationary domain. The rotating domain is a cylinder that encloses the blades and the hub as shown in Figure 3.4. The domain size used was 1.1D for the diameter and 0.4D for the thickness of the rotating domain and 8D for width, height and length of the stationary domain (Kutty & Rajendran, 2017). The domain size was selected as follows so that no recirculation of flow occurs in the domain and any convergence problem exist because the upstream and downstream may affect the flow (Ansys, 2006).The simulation was conducted with different advance ratios and velocities as shown in Table 3.2

Table 3.2: Advance ratio and inlet velocity

Advance Ratio	Velocity Inlet (m/s)
0.236	2.9972
0.334	4.2418
0.432	5.4864
0.527	6.6929
0.573	7.2771
0.628	7.9756
0.717	9.1059

3.6 Mesh Generation

Mesh plays an important role to get an accurate result (Chen et al., 2020). The grid was generated using the meshing module in ANSYS FLUENT 18.2. A tetrahedral mesh was used in this simulation due to the complex shape of the blades. The tetrahedral mesh was denser at the rotating domain and less dense at the global stationary domain for a better fluid flow result. The mesh was generated with six types of quality: standard, coarse, mid, mid-fine, fine, and extremely fine. Table 3.3 shows the details of the mesh grid generation. Figure 3.5 shows the surface mesh of the propeller blade.

Table 3.3: Mesh generation data

Size function	Proximity and Curvature
Relevance centre	Fine
Max face size	2.5 e-2 m
Growth rate	1.20
Span Angle Centre	Fine
Minimum Size	5.138e-4 m
Maximum Tetrahedral Size	0.102760 m
Curvature normal angle	40 degree
Proximity minimum size	5.138e-4 m
Minimum Edge length	1.7812e-4 m

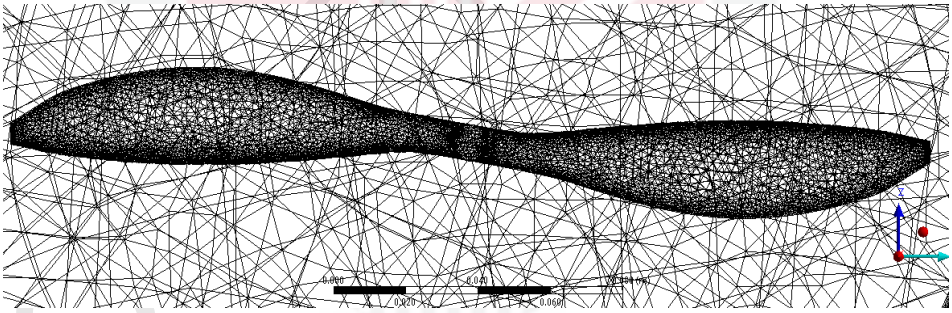

Figure 3.7: The surface mesh of the propeller blade and rotating domain.

Mesh dependency test was conducted to determine the optimised number of meshing for the simulation study (Figure 3.6). Figure 3.6 shows the results of the mesh dependency test from 0 to 9 million number of mesh element. The results showed that the 3 million number of an element is the best number of mesh for the study which can optimize the simulation duration and without affecting the computational accuracy.

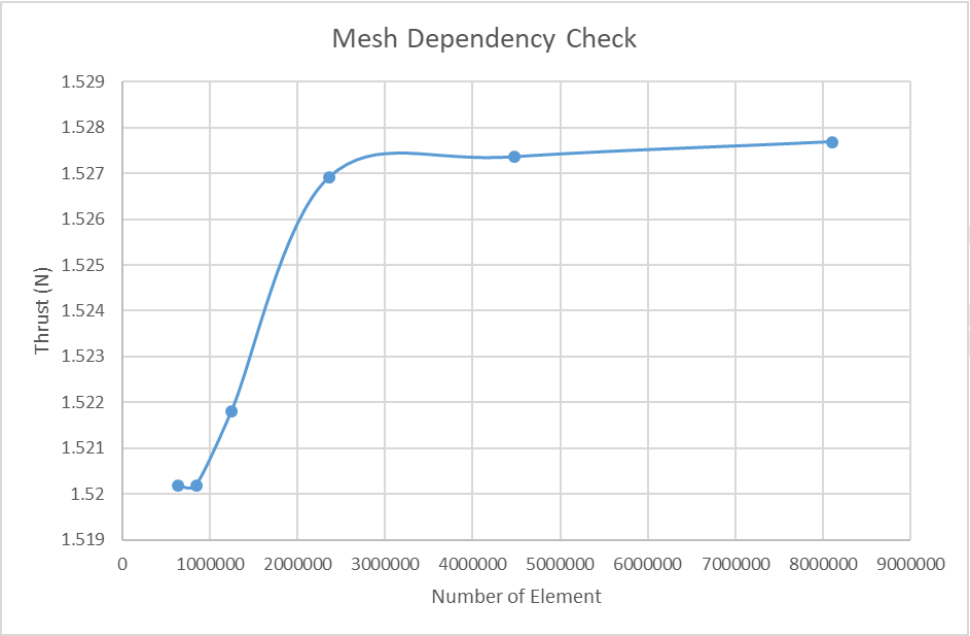

Figure 3.8: Mesh dependency test

3.7 Boundary Condition

The CFD simulation was conducted in the flow condition as shown in Table 3.2 with a fixed rotation speed of 3008 RPM. The freestream velocity with 0.1% turbulent intensity was used as the inlet boundary and the outlet boundary was set to be outflow condition similar to the work done by (Deters et al., 2014). A no-slip condition was set on all the walls of the domain. The rotating domain that enclosed the propeller blade was assigned with MRF, so that it can be rotated with the desired rotational speed. Six turbulence models were used to obtain an accurate result for the simulation. The Reynolds number of the propeller was calculated at approximately 50,804 and the residual error of $1x10^{6}$ to obtain the accurate result.

Furthermore, to obtain accurate results, several other important aspects in terms of boundary conditions were considered in this simulation. The pressure-velocity coupling solution was set to be a Semi-Implicit Method for Pressure-Linked Equations (SIMPLE). The first order selection was used for Turbulent Kinetic Energy and Turbulent Dissipation Rate solution. Meanwhile, for momentum and pressure solution, the second order was selected and the least square Cell-based Algorithm was employed for the gradient solution sets.

3.8 Time Dependency-Check

As the simulation is transient, a time-step dependency test was required to be performed to determine the best time-step size, thus minimising time consumption in computational analysis. In this study, 3008 RPM was used for the rotational domain with 50.13 revolutions per second. Five time-step sizes were studied in this study where the results showed 0.02s is the best time step required for 50 iterations to complete one simulation (refer Figure 3.7).

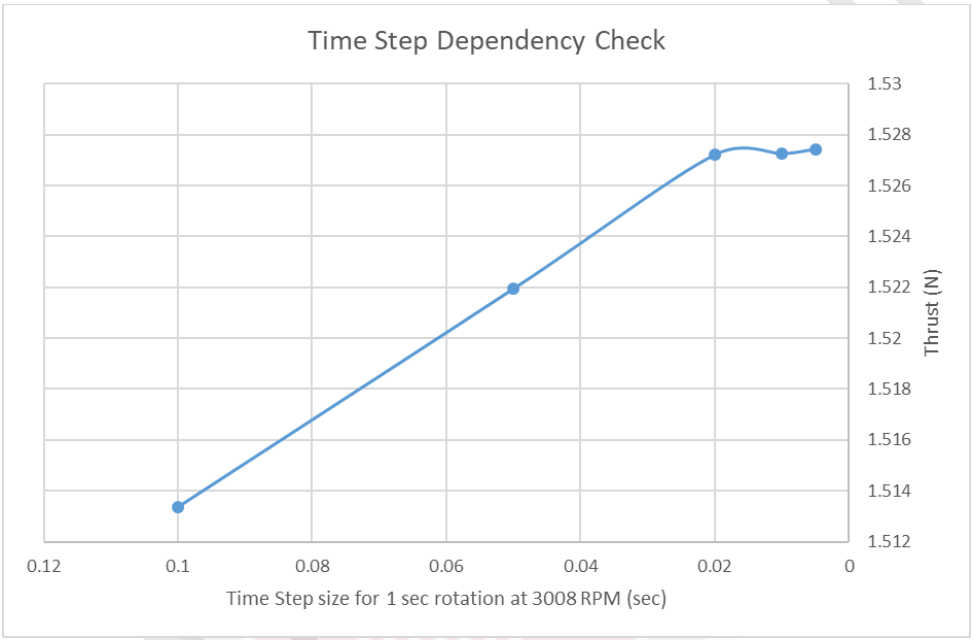

Figure 3.9: Time dependency check

3.9 Turbulence Model Selection

In this study, the turbulence model selection was examined for producing accurate and reliable result subjected to the experimental data. Referring to Table 4.1, six turbulence models (k-ε standard, k-ε RNG, k-ε realizable, k-ω normal, k-ω BSL, and k-ω SST) were analysed to determine the best turbulence model for the simulations. The percentage difference of thrust coefficient between each turbulence model was compared to determine the most accurate result subjected to the experimental data. From the results obtained, k-ω normal showed the best turbulence model due to the lowest percentage difference compared to the other models with 1.1249%. Hence, in this study, k-ω normal was selected as the best turbulent model to be used for low Reynold's number as supported by (Kutty & Rajendran, 2017).

Table 3.4: Turbulence model and percentage difference

Turbulance Model	Percentage Difference (%)
K-Epsilon (Standard)	2.039639523
K-Epsilon (RNG)	3.558895773
K-Epsilon (Realizable)	3.640422185
K-Omega (Normal)	1.124981088
K-Omega (BSL)	1.210208456
K-Omega (SST)	1.762005129

3.10 Summary

In this study FVM has been selected for the CFD solver and this analysis utilze MRF with the help of ANSYS Fluent 18.2 software. The propellers were designed by changing the AOP at each blade station which produced a different design of propeller shape which can be referred to in percentage of 0% AOP, 25% AOP, 50% AOP, 75% AOP, and 100% AOP. There are two domains which are rotational domain that enclosed the propeller and will be assigned with MRF at 3008 revolutions per minute and a stationary domain that act as inlet velocity and outlet. Multiple Reference Frame (MRF) technique was used for the rotation of the propeller subjected to its local reference frame at 3008 revolutions per minute (RPM). A tetrahedral mesh with the number of elements of 3 million was used for this analysis with time step of 0.02.

The result will be first validated and later proper design improvement was made. The thrust power and efficiency of the design improvement were compared to the original design to see are there any improvement of the design. The variables of thrust, T (N), torque, Q (N.m), the rotational speed of propeller, n (rps), the diameter of propeller, D (m), the density of the fluid, ρ (kg.m-3), and power, P (W) were determined via the CFD analysis. Then, the results of thrust coefficient (Ct), torque coefficient (Cq), power coefficient (Cp), advance ratio (J), and efficiency (η) were calculated using the following equations (1-5). The relative percentage error of Ct, Cq and η can be calculated by equation (6-8) (Brandt & Selig, 2011).

$$C_T = \frac{T}{\rho n^2 D^4} \quad (1)$$

$$C_Q = \frac{Q}{\rho n^2 D^5} \quad (2)$$

$$C_P = \frac{P}{\rho n^3 D^5} \quad (3)$$

$$J = \frac{V}{nD} \quad (4)$$

$$\eta = \frac{C_T J}{C_P} \quad (5)$$

$$\Delta C_T(\%) = (C_{T_{CFD}} - C_{T_{EXP}})/C_{T_{EXP}} \times 100 \quad (6)$$

$$\Delta C_T(\%) = (C_{T_{CFD}} - C_{T_{EXP}})/C_{T_{EXP}} \times 100 \quad (7)$$

$$\Delta\eta(\%) = (\eta_{CFD} - \eta_{EXP})/\eta_{EXP} \times 100 \quad (8)$$

CHAPTER 4

RESULTS AND DISCUSSION

4.1 Introduction

In this chapter, the results are presented. There are two types of results that will be presented which are qualitative and quantitative data. The simulation was validated with the experimental and manuscript previous data. This is mandatory in researching using computational method in order to have consistent results and also the results are accurate and reliable. After that design improvement was made to see either the new design will provide improvement or not.

4.2 Validation with experimental and manuscript data

Further, the validation study between experimental data of the APC Slow Flyer propeller blade (Engineering | APC Propellers, n.d.) and CFD analysis was performed to determine the standard simulation methodology and accurate results between both approaches. The validation study between 0% AOP, 25% AOP propeller design and experimental data were performed by comparing the results of Cp, Ct and η to determine the optimum percentage of AOP of the propeller (Faris et al., 2020). Referring to Figure 4.1, the pattern of Cp, Ct and η showed a similar pattern between the CFD simulation of 0% AOP, 25% AOP and the experimental data. In details, the 25% AOP showed the most accurate results compared to the 0% AOP subjected to the experimental data. The average percentage difference of Cp, Ct and η were stated to be 9.80%, 14.09% and 3.06% for 25% AOP, respectively compared to the 0% AOP with 12.13%, 16.37% and 3.87%. Hence, it is proven that the 25% AOP produced the most accurate result when compared to the experimental data which supported the validation study.

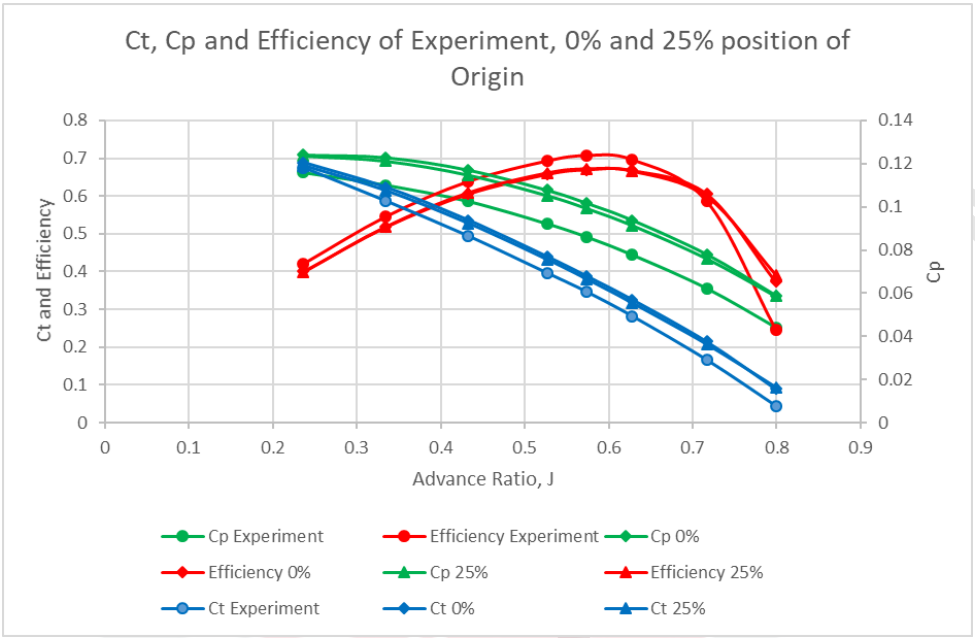

Figure 4.1: Ct, Cp and Efficiency of Experiment, 0% and 25% position of Origin.

4.3 Design Improvement

Further, the propeller design improvement with 50% AOP, 75% AOP and 100% AOP were simulated to investigate the effect of changing AOP percentage on the aerodynamics performance in terms of coefficient of thrust, coefficient of power, and its efficiency.

4.3.1 Coefficient of Thrust

Figure 4.2 showed the coefficient values of thrust, Ct for 25% AOP, 50% AOP, 75% AOP and 100% AOP at different advance ratio value. Meanwhile, Table 4.2 indicated the detailed Ct value of each parameter and percentage error between 50% AOP, 75% AOP and 100% AOP with respect to 25% AOP. Referring the Figure 4.2, it can be observed that the pattern of the graph for all AOP percentage showed a similar pattern with small differences. The Ct value stated to be high at 0.236 advance ratio and the value reduced towards a higher advance ratio of 0.799. Meanwhile, referring to Table 4.2, it can be observed that the 75% AOP produced the highest percentage difference of Ct at each advance ratio when compared to 50% AOP and 100% AOP. For the advance ratio of 0.236, 75% AOP produced the higher percentage difference with 1.440% followed with the 100% AOP and 50% AOP with 1.260% and 0.875%, respectively. At the highest advance ratio value of 0.799, the percentage difference of 50% AOP showed the lowest value with 0.523% followed by the 100% AOP with 7.473%. Hence, the 75% AOP indicate the highest percentage difference value with 7.818%. It can be concluded, the

75% AOP produced better Ct performance with the highest increment value than the others.

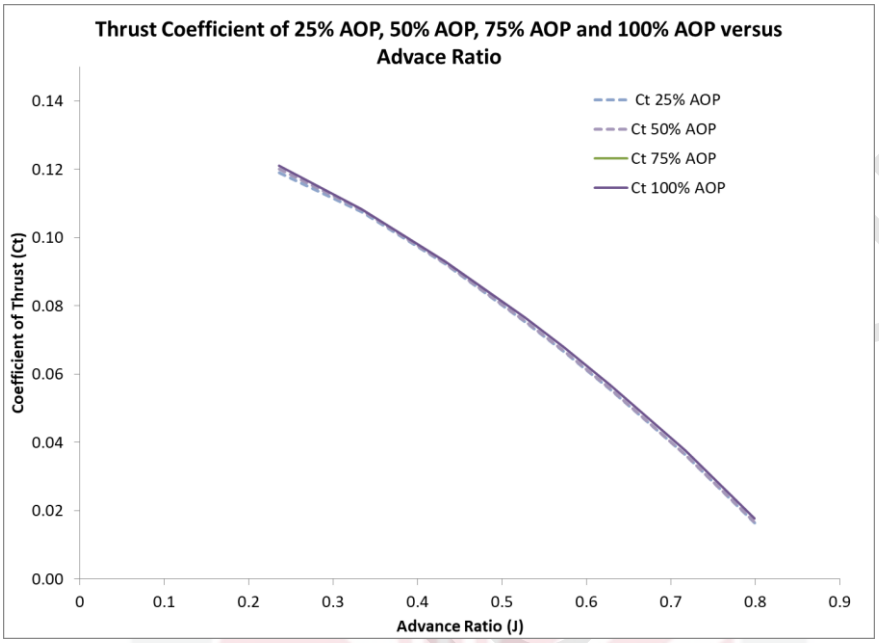

Figure 4.2: Ct performance of 25% AOP, 50% AOP, 75% AOP and 100% AOP

Table 4.1: Ct percentage difference of 50% AOP, 75% AOP and 100% AOP with respect 25% AOP

Advance Ratio (J)	Ct percentage difference.		
J	**50%**	**75%**	**100%**
0.236	0.875	1.440	1.260
0.334	0.472	0.990	0.663
0.432	0.277	1.169	0.754
0.527	0.167	1.536	1.474
0.573	0.140	1.828	1.187
0.628	0.333	2.491	2.464
0.717	0.114	0.598	0.119
0.799	0.523	7.818	7.473

4.3.2 Coefficient of power

Figure 4.3 showed the coefficient values of power, Cp for 25% AOP, 50% AOP, 75% AOP and 100% AOP at different advance ratio value. Meanwhile, Table 4.3 indicated the

details Cp value of each parameter and percentage error between 50% AOP, 75% AOP and 100% AOP with respect to 25% AOP. The pattern of the graph (in Figure 4.3) for all AOP percentage showed a similar pattern with small differences for lower and higher advance ratio. At the lowest advance ratio of 0.236, the Cp value of 50% AOP, 75% AOP and 100% AOP showed a higher value than the 25% AOP. However, the Cp showed a reduction value towards a higher advance ratio of 0.799 where the 25% AOP indicate a higher value than the others. In details, by referring to Table 4.3, it can be observed that the 75% AOP produced the positive value of Cp percentage difference at advance ratio 0.236 to 0.527 with respect to 25% AOP. However, at an advance ratio of 0.573 to 0.799, all AOP showed a reduction of Cp value with a negative percentage difference with respect to 25% AOP. At the highest advance ratio value of 0.799, the percentage difference of 100% AOP showed the highest reduction percentage difference value with -5.587% followed by 50% AOP and 75% AOP with -3.599% and -2.682%, respectively. It can be concluded, the 100% AOP produced better Cp performance with the highest reduction value than the others.

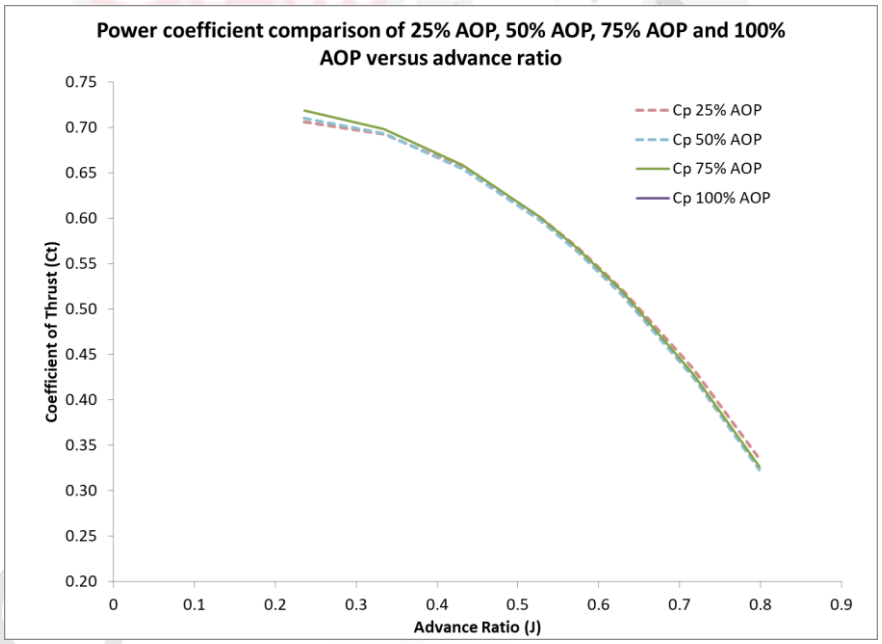

Figure 4.3: Cp performance of 25% AOP, 50% AOP, 75% AOP and 100% AOP

Table 4.2: Coefficient of power design improvement percentage difference with respect to 25%AOP

	Cp percentage difference with respect to 25%AOP		
J	**50%**	**75%**	**100%**
0.236	0.577	1.700	1.521
0.334	0.039	0.745	0.360
0.432	-0.267	0.367	-0.138

Table 4.2: Continued

0.527	**-0.605**	**0.034**	**-0.283**
0.573	-0.821	-0.158	-0.469
0.628	-1.172	-0.515	-0.957
0.717	-2.196	-1.489	-2.615
0.799	-3.599	-2.682	-5.587

4.3.3 Efficiency

Furthermore, Figure 4.4 showed the efficiency, η for 25% AOP, 50% AOP, 75% AOP and 100% AOP at different advance ratio value. Meanwhile, Table 4.4 indicated the details η value of each parameter and percentage error between 50% AOP, 75% AOP and 100% AOP with respect to 25% AOP. The pattern of the graph (in Figure 4.4) for all AOP percentage showed a similar pattern with small differences for the lower advance ratio and showed significant difference towards the higher advance ratio. At the advance ratio of 0.236 to 0.527, the η value of 50% AOP, 75% AOP and 100% AOP showed a small difference value when compared to the 25% AOP. However, the efficiency graph showed a significant difference towards a higher advance ratio and reach its peak at 0.717 where the 100% AOP indicate a higher value than the others. In details, by referring to Table 4.4, it can be observed that the 100% AOP produced the highest efficiency percentage difference with respect to 25% AOP at every advance ratio compared to the 50% AOP and 75% AOP. At the advance ratio of 0.799, the percentage difference of 100% AOP showed the highest percentage difference value with 15.891% followed by 75% AOP and 50% AOP with 15.674% and 4.277%, respectively when respect to 25% AOP. It can be concluded, the 100% AOP produced better η performance with the highest efficiency percentage compared to the others.

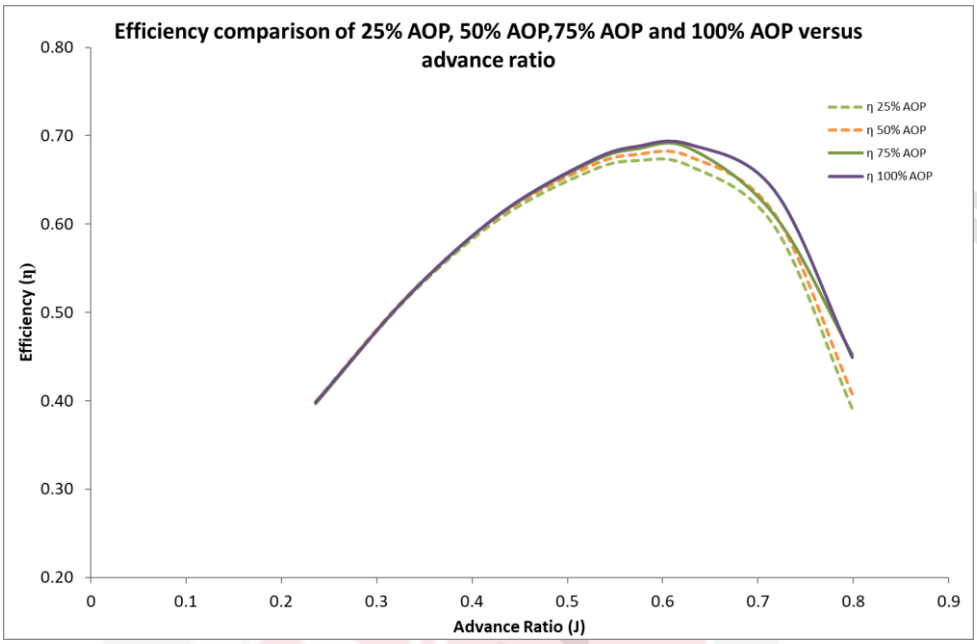

Figure 4.4: Effeciency performance of 25% AOP, 50% AOP, 75% AOP and 100% AOP

Table 4.3: Coefficient of thrust design improvement percentage difference with respect to 25% AOP

	Efficiency percentage difference with respect to 25% AOP		
J	**50%**	**75%**	**100%**
0.236	0.295	0.252	0.137
0.334	0.433	0.243	0.302
0.432	0.546	0.798	0.894
0.527	0.777	1.500	1.762
0.573	0.969	1.989	2.399
0.628	1.524	3.022	3.656
0.717	2.362	2.118	6.811
0.799	4.277	15.674	15.891

4.4 Discussion

From the analysis of the results, it can be observed that the 75% AOP produced the highest Ct compared to the 25% AOP, 50% AOP and 100% AOP. However, the Cp results showed that the 100% AOP produce the lower value of power compared to the other. Hence, a better comparison study can be made based on the efficiency results between all propellers design where the 100% AOP produced the highest efficiency results

followed by 75% AOP, 50% AOP and 25% AOP. It can be observed that the changes of the position of origin affected the shape of the propeller blade and produced significant changes in the aerodynamics perspective. For example, referring to Figure 4.5, the 25% AOP at each station produced a down shape of propeller blade compared to the 100% AOP where the propeller blade created the upper shape of the propeller blade. Hence, increasing the percentage of AOP at each station changes the design and lead towards an upper shape propeller blade. Furthermore, this change has affected the fluid flow behaviour which enhances the aerodynamics performance of the propeller blade at the rotational speed of 3008 rpm.

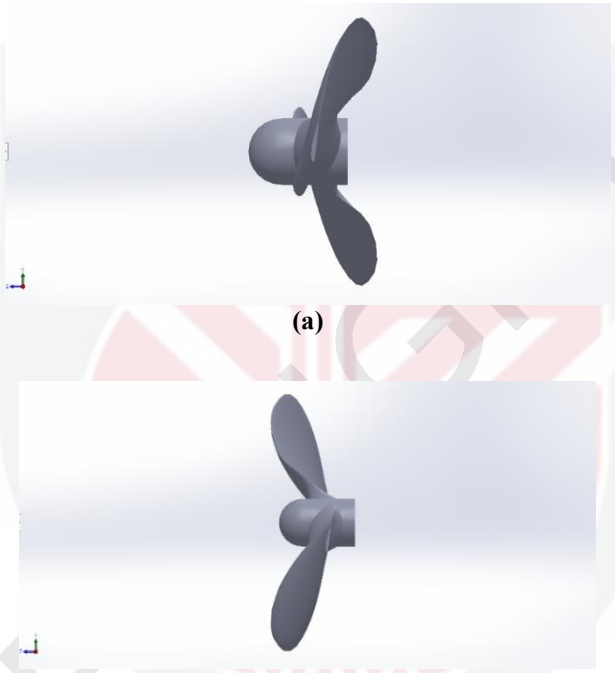

Figure 4.5: APC Slow Flyer propeller blade of (a) 25% AOP (b) 100% AOP

This showed that several things can be investigated to determine the reason behind the slight increment value in the thrust when the position of origin is increased. Velocity and pressure are two related and important parameters that provide lift or thrust to the propeller. Bernoulli's principle states that an increase in a liquid's speed creates a decrement pr pressure magnitude and a decrement in a liquid's speed creates an increment of pressure magnitude. Figure 4.6 represent the velocity contour of 25% AOP, 50 % AOP, 75% AOP and 100% AOP. Quantitatively, the 100% AOP produced the highest velocity magnitude with 44.22 m/s followed by 25% AOP, 75% AOP, and 50% AOP with 44.20 m/s, 44.08 m/s and 44.04 m/s, respectively. Even though quantitative results do not show major changes, however, on a qualitative perspective, the velocity distribution of 100% AOP along with the propeller from the tips to the centre of the hub

showed better distribution compared to the others. This will lead to the improvement of fluid flow performance compared to the others AOP propeller design due to the enhanced aerodynamics shape of the propeller.

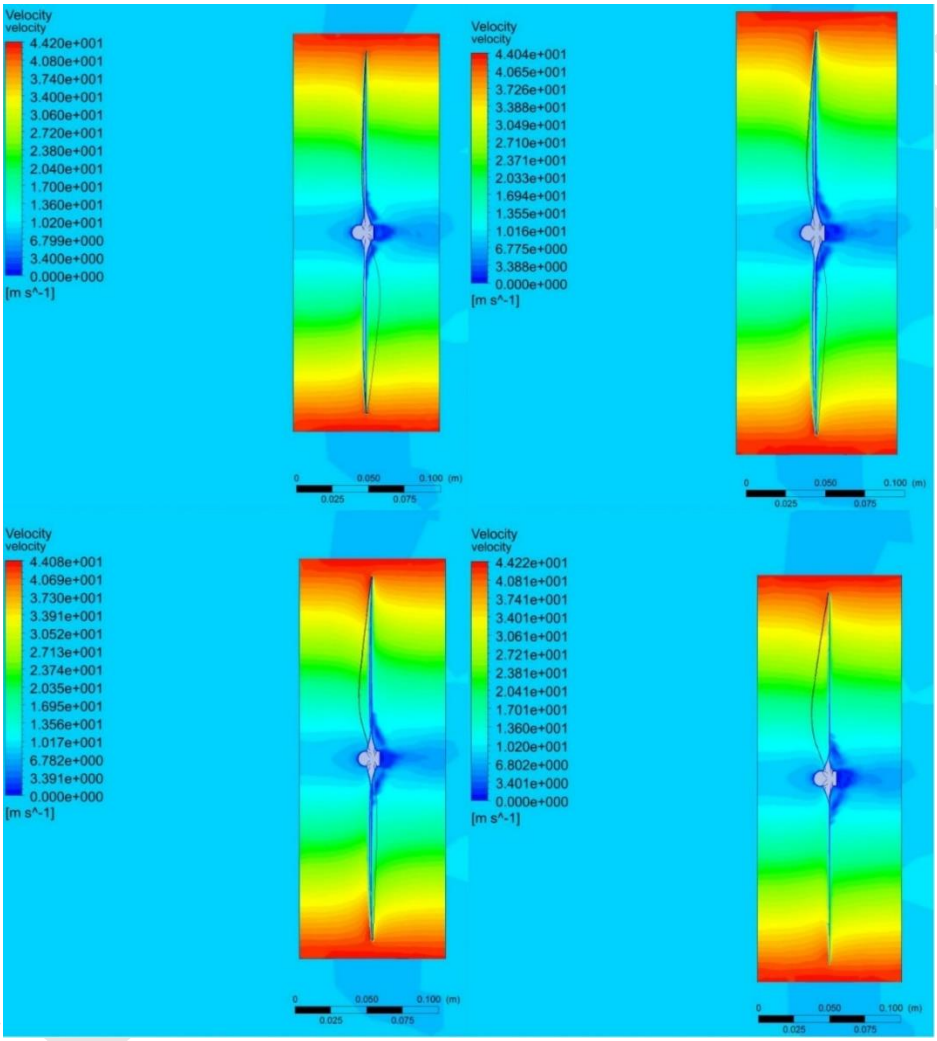

Figure 4.6: Velocity contour of APC Slow Flyer propeller blade of (a) 25% AOP (b) 50% AOP (c) 75% AOP (d) 100% AOP

The effects of changing the AOP showed that the maximum and minimum pressure value increased when the position of origin increased. The results demonstrated that at 25% AOP, the minimum and maximum values of pressure were -238.20 Pa and 67.89 Pa, respectively. At the 50% AOP, the minimum and maximum values were -277.00 Pa and 164.00 Pa, respectively. At 75% AOP, the minimum and maximum values of pressure increased to -300.20 Pa and 225.50Pa, respectively. As the airfoil origin position increased to 100% AOP, a huge pressure difference was stated between the minimum and maximum value with -669.20 Pa and 436.70 Pa, respectively. Referring to Figure

4.7, it can be observed that the minimum pressure value occurred upstream of the blade, while the maximum pressure value occurred downstream of the propeller for each AOP percentage. This indicates a higher pressure acting at the downstream of the blade and lower pressure acting at the upstream of the blade produced thrust force for the lifting purposes of a drone. Hence, the major differences of pressure value for 100% AOP have led to the best efficiency of airfoil origin position where it produced a high value of thrust with a low magnitude of power consumption.

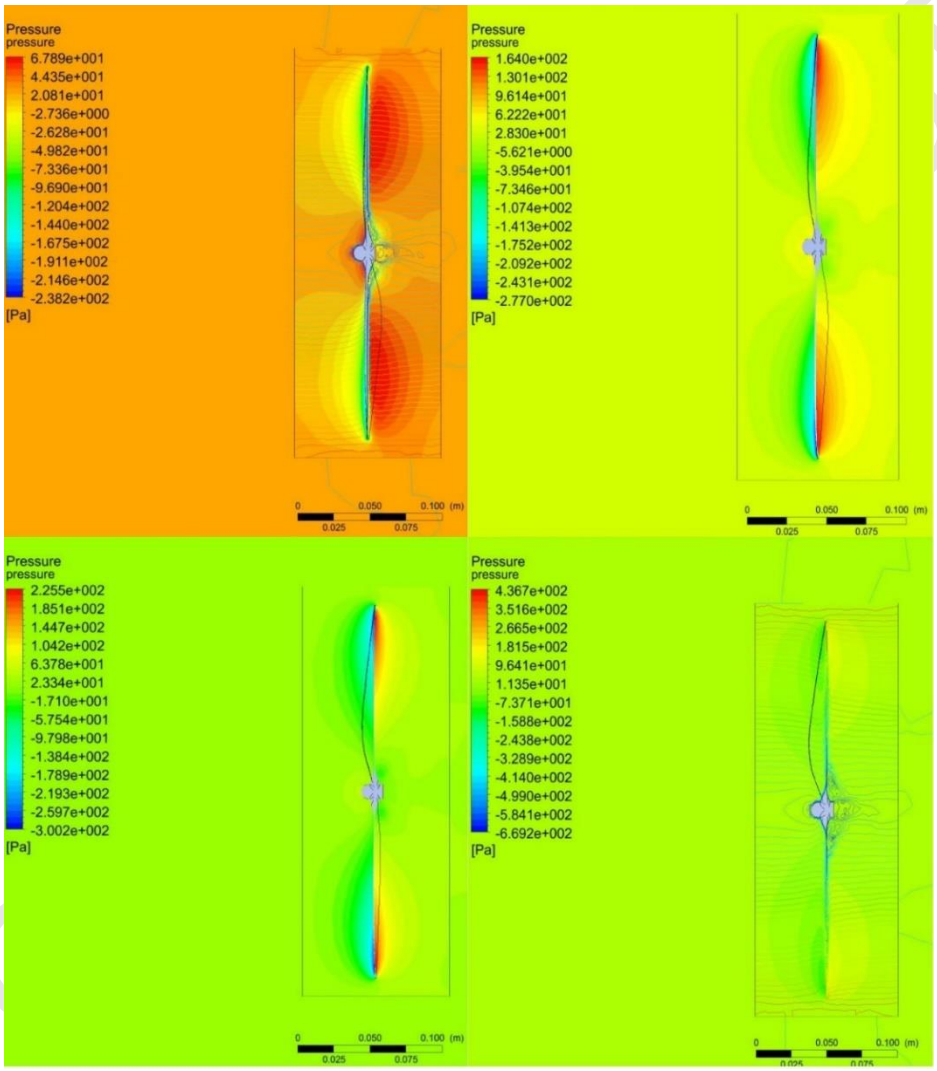

Figure 4.7: Pressure contour of APC Slow Flyer propeller blade of (a) 25% AOP (b) 50% AOP (c) 75% AOP (d) 100% AOP

REFERENCES

A. Amiri, H., Shafaghat, R., Alamian, R., Taheri, S. M., & Safdari Shadloo, M. (2019). Study of horizontal axis tidal turbine performance and investigation on the optimum fixed pitch angle using CFD: A case study of Iran. *International Journal of Numerical Methods for Heat and Fluid Flow*. https://doi.org/10.1108/HFF-05-2019-0447

Ali, M. I. M., Afandi, A. N., & Bardai, A. M. (2019). Analysis on propeller design for medium-sized drone (DJI phantom 3). *International Journal of Innovative Technology and Exploring Engineering*, *8*(7), 217–221.

Andrés, P. G., Lopez, O., Poroseva, S. V., & Escobar, J. A. (2019). Computational study of a small rotor at hover using CFD and UVLM. *AIAA Scitech 2019 Forum*, *January*, 1–14. https://doi.org/10.2514/6.2019-0597

Anemaat, W. A. J., Schuurman, M., Liu, W., & Karwas, A. (2017). Aerodynamic design, analysis and testing of propellers for small unmanned aerial vehicles. *AIAA SciTech Forum - 55th AIAA Aerospace Sciences Meeting*, *January*, 1–12. https://doi.org/10.2514/6.2017-0721

Ansys. (2006). Modeling of Turbulent Flows. *Fluent User Guide*. chrome-extension://oemmndcbldboiebfnladdacbdfmadadm/http://www.southampton.ac.uk/~nwb/lectures/GoodPracticeCFD/Articles/Turbulence_Notes_Fluent-v6.3.06.pdf

Asson, K. M., & Dunnt, P. F. (1991). *Determine Propeller Performance*. *29*(1), 1–2.

Barnitsas, M. M., Ray, D., & Kinley, P. (2012). *Kt, Kq and Efficiency Curves for the Wageningen B-Series Propellers*.

Ben Nasr, N., Falissard, F., Decours, J., Gavériaux, R., Delrieux, Y., Canard-Caruana, S., Laban, M., Brouwer, H. H., Albrecht, M., Scholz, C., Diette, C., & Chartrain, D. (2017). Propeller analysis using low & high fidelity aero-acoustic methods. *35th AIAA Applied Aerodynamics Conference, 2017*, *June*, 1–13. https://doi.org/10.2514/6.2017-3573

Brandt, J. B., & Selig, M. S. (2011). Propeller Performance Data at Low Reynolds Numbers. *AIAA Aerospace Science Proceeding*, *January*, 1–18.

Brouwer, H. H. (1992). On the use of the method of matched asymptotic expansions in propeller aerodynamics and acoustics. *Journal of Fluid Mechanics*, *242*, 117–143. https://doi.org/DOI: 10.1017/S0022112092002301

Cambier, L., Heib, S., & Plot, S. (2013). The Onera elsA CFD software: Input from research and feedback from industry. *Mechanics and Industry*, *14*(3), 159–174. https://doi.org/10.1051/meca/2013056

Chan, W. M. (2002). *AIAA 2002-3188 THE OVERGRID INTERFACE FOR COMPUTATIONAL SIMULATIONS ON OVERSET GRIDS 32nd AIAA Fluid*

Dynamics Conference 24-26 June , 2002 / St . Louis , Missouri.

Chen, X., Liu, J., Pang, Y., Chen, J., Chi, L., & Gong, C. (2020). Developing a new mesh quality evaluation method based on convolutional neural network. *Engineering Applications of Computational Fluid Mechanics*, *14*(1), 391–400. https://doi.org/10.1080/19942060.2020.1720820

Colmenares, J. D., López, O. D., & Preidikman, S. (2015). Computational Study of a Transverse Rotor Aircraft in Hover Using the Unsteady Vortex Lattice Method. *Mathematical Problems in Engineering*, *2015*, 478457. https://doi.org/10.1155/2015/478457

Derakhshan, S. ., & Mostafavi, A. (2011). Optimization of GAMM Francis Turbine Runner. *International Scholarly and Scientific Research & Innovation*, *5*(11), 11–26.

Derakhshan, S., Tavaziani, A., & Kasaeian, N. (2015). Numerical Shape Optimization of a Wind Turbine Blades Using Artificial Bee Colony Algorithm. *Journal of Energy Resources Technology*, *137*(5), 1–12. https://doi.org/10.1115/1.4031043

Deters, R. W., Ananda, G. K., & Selig, M. S. (2014). Reynolds number effects on the performance of small-scale propellers. *32nd AIAA Applied Aerodynamics Conference*, *June*, 1–43. https://doi.org/10.2514/6.2014-2151

Drela, M. (1989). XFOIL: an analysis and design system for low Reynolds number airfoils. *Low Reynolds Number Aerodynamics. Proc. Conf., Notre Dame, U.S.a., June 5-7, 1989 }Edited By T.J. Mueller]. (Lecture Notes In*, *54)*, *Berlin*, *Germany*, *Springer-Verlag*, *1989*, 1–12. https://doi.org/10.1007/978-3-642-84010-4_1

Drzewiecki, S. (1920). *Théorie générale de l'hélice : hélices aériennes et hélices marines*. Paris, : Gauthier-Villars et cie.

Eltayesh, A., Hanna, M. B., Castellani, F., Huzayyin, A. S., El-Batsh, H. M., Burlando, M., & Becchetti, M. (2019). Effect of wind tunnel blockage on the performance of a horizontal axis wind turbine with different blade number. *Energies*, *12*(10), 1–15. https://doi.org/10.3390/en12101988

Engineering | APC Propellers. (n.d.). Retrieved January 6, 2020, from https://www.apcprop.com/technical-information/engineering/#airfoil

Fernandes, S. D. (2017). *Performance Analysis of a Coaxial Helicopter in Hover and Performance Analysis of a Coaxial Helicopter in Hover and Forward Flight Forward Flight Scholarly Commons Citation Scholarly Commons Citation*. https://commons.erau.edu/edt

Future of Drones: Applications & Uses of Drone Technology in 2021. (n.d.). Retrieved September 30, 2021, from https://www.businessinsider.com/drone-technology-uses-applications

Goldstein, S. (1929). On the Vortex Theory of Screw Propellers. *Proceedings of the Royal Society of London. Series A, Containing Papers of a Mathematical and*

Physical Character, *123*(792), 440–465. http://www.jstor.org/stable/95206

Han, H., Xiang, C., Xu, B., & Yu, Y. (2017). Experimental and computational analysis of microscale shrouded coaxial rotor in hover. *2017 International Conference on Unmanned Aircraft Systems, ICUAS 2017*, 1092–1100. https://doi.org/10.1109/ICUAS.2017.7991413

Havill, C. H. (1929). Aircraft propellers. *SAE Technical Papers*, *970*, 460–466. https://doi.org/10.4271/290059

Hrishikeshavan, V., Black, J., & Chopra, I. (2012). Development of a quad shrouded rotor micro air vehicle and performance evaluation in edgewise flow. *Annual Forum Proceedings - AHS International*, *1*, 665–684.

Ianniello, S., & National, I. (2015). *Theoretical Modelling of Unsteady Cavitation and Induced Noise THEORETICAL MODELLING OF UNSTEADY CAVITATION AND INDUCED NOISE*. *August*.

Karczewski, M., & Eglin, P. (2014). Application of the modified blade element method for propeller blade design on high-speed helicopter X3. *Zeszyty Naukowe. Cieplne Maszyny Przepływowe - Turbomachinery / Politechnika Łódzka*, *nr 145*, 63–64.

Kuantama, E., & Tarca, R. (2017). Quadcopter thrust optimization with ducted-propeller. *MATEC Web of Conferences*, *126*, 1–4. https://doi.org/10.1051/matecconf/201712601002

Kutty, H. A., & Rajendran, P. (2017a). *3D CFD Simulation and Experimental Validation of Small APC Slow Flyer Propeller Blade*. https://doi.org/10.3390/aerospace4010010

Kutty, H. A., & Rajendran, P. (2017b). Review on numerical and experimental research on conventional and unconventional propeller blade design. *International Review of Aerospace Engineering*, *10*(2), 61–73. https://doi.org/10.15866/irease.v10i2.11547

Kwon, H. Il, Yi, S., Choi, S., & Kim, K. (2015). Design of efficient propellers using variable-fidelity aerodynamic analysis and multilevel optimization. *Journal of Propulsion and Power*, *31*(4), 1057–1072. https://doi.org/10.2514/1.B35097

Kwon, H. Il, You, J. Y., & Kwon, O. J. (2012). Enhancement of wind turbine aerodynamic performance by a numerical optimization technique. *Journal of Mechanical Science and Technology*, *26*(2), 455–462. https://doi.org/10.1007/s12206-011-1035-2

Lee, S. (1998). *PROPELLER BLADE SHAPE OPTIMIZATION FOR EFFICIENCY IMPROVEMENT*. *27*(3), 407–419.

Malmir, R. (2019). A CFD study on the correlation between the skew angle and blade number of hydrodynamic performance of a submarine propeller. *Journal of the Brazilian Society of Mechanical Sciences and Engineering*, *41*(8). https://doi.org/10.1007/s40430-019-1822-8

McCrink, M. H., & Gregory, J. W. (2017). Blade element momentum modeling of low-reynolds electric propulsion systems. *Journal of Aircraft*, *54*(1), 163–176. https://doi.org/10.2514/1.C033622

Merchant, M. P. (2005). *Propeller performance measurement for low Reynolds number unmanned aerial vehicle applications. December*.

Milne-Thomson, L. M. (2011). *Theoretical Aerodynamics (Dover Books on Aeronautical Engineering)*. Dover Publications. http://www.amazon.com/exec/obidos/redirect?tag=citeulike07-20&path=ASIN/048661980X

Molina-Aiz, F. D., Fatnassi, H., Boulard, T., Roy, J. C., & Valera, D. L. (2010). Comparison of finite element and finite volume methods for simulation of natural ventilation in greenhouses. *Computers and Electronics in Agriculture*, *72*(2), 69–86. https://doi.org/10.1016/j.compag.2010.03.002

Morgado, J., Abdollahzadeh, M., Silvestre, M. A. R., & Páscoa, J. C. (2015). High altitude propeller design and analysis. *Aerospace Science and Technology*, *45*, 398–407. https://doi.org/10.1016/j.ast.2015.06.011

NASA. (2010). Bernoulli ' s Principle principles of flight. *Museum in the BOX*, 38 pages. https://www.nasa.gov/sites/default/files/atoms/files/bernoulli_principle_k-4.pdf

Nouri, N. M., & Mohammadi, S. (2016). A multi-objective approach for determining the number of blades on a NACA marine propeller. *Brodogradnja*, *67*(2), 15–32. https://doi.org/10.21278/brod67202

Peng, W., Li, G., Geng, J., & Yan, W. (2019). A strategy for the partition of MRF zones in axial fan simulation. *International Journal of Ventilation*, *18*(1), 64–78. https://doi.org/10.1080/14733315.2018.1431361

Pulliam, T. H. (2011). High order accurate finite-difference methods: As seen in OVERFLOW. *20th AIAA Computational Fluid Dynamics Conference 2011*, *June*, 1–14. https://doi.org/10.2514/6.2011-3851

Selig, M. S., & McGranahan, B. D. (1995). Summary of Low speed Airfoil Dara - Vol 1. In *Uicc* (Vol. 1). https://doi.org/10.1115/1.1793208

Silvestre, M. A. R., Morgado, J., & Páscoa, J. C. (2013). JBLADE: A propeller design and analysis code. *2013 International Powered Lift Conference*, 1–12. https://doi.org/10.2514/6.2013-4220

Sobieczky, H. (1999). *Parametric Airfoils and Wings* (Vol. 68, pp. 71–87). https://doi.org/10.1007/978-3-322-89952-1_4

Somers, D. M. (1997). *Design and Experimental Results for the S809 Airfoil*. *January 1997*, 104. https://doi.org/10.2172/437668

Spera, D. A. (2009). *Wind turbine technology : fundamental concepts of wind turbine*

engineering. ASME Press.

Stajuda, M., Karczewski, M., Obidowski, D., & Jóźwik, K. (2016). Development of a CFD model for propeller simulation. *Mechanics and Mechanical Engineering*, *20*(4), 579–593.

Stan, L.-C. D. (2019). *Optimization by CFD of the marine propulsion system*. *January*, 96. https://doi.org/10.1117/12.2324418

Stepniewski, W. Z., & Keys, C. N. (1984). *Rotary-wing aerodynamics.* Dover Publications. http://search.ebscohost.com/login.aspx?direct=true&scope=site&db=nlebk&db=nlabk&AN=1152401

Subhas, S., Saji, V. F., Ramakrishna, S., & Das, H. N. (2012). CFD analysis of a propeller flow and cavitation. *International Journal of Computer Applications in Technology*, *55*(16), 26–33. https://doi.org/10.5120/8841-3125

Sudarsono, Purwanto, & Wahyuadi, J. (2013). Optimization design of airfoil propellers of modified NACA 4415 using computational fluids dynamics. *Advanced Materials Research*, *789*, 403–407. https://doi.org/10.4028/www.scientific.net/AMR.789.403

Traub, L. W. (2016). Simplified propeller analysis and design including effects of stall. *Aeronautical Journal*, *120*(1227), 796–818. https://doi.org/10.1017/aer.2016.31

Turner, R. S. A. (2010). *Design and Optimisation of a Propeller for a Micro Air Vehicle Using Computational Fluid Dynamics Table of Contents*.

Van Treuren, K. W. (2015). Small-Scale Wind Turbine Testing in Wind Tunnels Under Low Reynolds Number Conditions. *Journal of Energy Resources Technology*, *137*(5). https://doi.org/10.1115/1.4030617

Yang, Y., Guo, Z., Song, Q., Zhang, Y., & Li, Q. (2018). Effect of blade pitch angle on the aerodynamic characteristics of a straight-bladed vertical axis wind turbine based on experiments and simulations. *Energies*, *11*(6). https://doi.org/10.3390/en11061514

Yang, Y., Guo, Z., Zhang, Y., Jinyama, H., & Li, Q. (2017). Numerical Investigation of the Tip Vortex of a Straight-Bladed Vertical Axis Wind Turbine with Double-Blades. In *Energies* (Vol. 10, Issue 11). https://doi.org/10.3390/en10111721

Yomchinda, T. (2018). Simplified propeller model for the study of uav aerodynamics using cfd method. *Proceedings of the 5th Asian Conference on Defence Technology, ACDT 2018*, 69–74. https://doi.org/10.1109/ACDT.2018.8592940

Yoon, S., Diaz, P. V., Boyd, D. D., Chan, W. M., & Theodore, C. R. (2017). Computational aerodynamic modeling of small quadcopter vehicles. *Annual Forum Proceedings - AHS International*, 371–386.